

THEORETICAL STUDY OF SECOND HARMONIC GENERATION OF A BLUE
LASER AT 486 *nm* USING A BBO CRYSTAL IN A
STANDING WAVE BUILD UP CAVITY

Ali Khademian, B.S.

Problems in Lieu of Thesis for the Degree of
MASTER OF SIENCE

UNIVERSITY OF NORTH TEXAS

May 2002

APPROVED:

David Shiner, Major Professor
Duncan Weathers, Minor Professor
Sam Matteson, Chair of the Physics Department
C. Neal Tate, Dean of the Robert B. Toulouse
School of Graduate Studies

Khademian, Ali, Theoretical Study of Second Harmonic Generation of a Blue Laser at 486 nm Using a BBO Crystal in a Standing Wave Buildup Cavity. Master of Science (Physics), May 2002, 60 pp, 22 figures, 5 tables, references, 21 titles.

For a spectroscopy purpose, we are interested in producing continuous wave (CW) UV laser light at 243 nm with at least 2 mW power. The theory of nonlinear optics suggests that we should be able to produce a desired 2.9 mW of 243 nm light by second harmonic generation (SHG) from a 50 mW blue laser at 486 nm using a BBO crystal in a build up cavity. The most important physical parameters are calculated. A 10 mm Brewster cut BBO crystal can provide phase matching conditions for coupling two ordinary photons at 486 nm and make a secondary beam at 243 nm. The single pass conversion efficiency is calculated not to be enough to generate 2.9 mW of SH light. My investigation shows that a standing wave build up cavity can provide a buildup factor of 94 and an overall conversion efficiency of 5.9% if one use an input coupler mirror with 1.1% transmission at 486 nm.

ACKNOWLEDGEMENT

I would like to thank David Shiner and Duncan Weathers who have helped me a great deal, understanding nonlinear optics and nonlinear crystal properties. And also I respectfully thank Bill Deering for his role in my partial understanding of the theory of electromagnetism.

TABLE OF CONTENTS

	Page
LIST OF FIGURES.....	v
LIST OF TABLES.....	vii
 Chapter	
1. INTRODUCTION.....	1
2. THEORY OF NONLINEAR OPTICS AND SECOND HARMONIC GENERATION.....	3
Linear Polarization	
Nonlinear Polarization	
Interaction of Two Optical Fields and SHG	
3. OPTICS OF UNIAXIAL CRYSTALS.....	11
Light Propagation in an Anisotropic Media	
Propagation of Light in Uniaxial Crystals	
Phase Matching Conditions for SHG in Uniaxial Crystals	
Two Different Types of Phase Matching for Negative Uniaxial Crystals	
The Effective Nonlinear Coefficient	
The Walkoff Phenomena	
The Single Pass Conversion Efficiency	
4. BUILDUP CAVITIES.....	41
Configurations of Buildup Cavities Using Mirrors	

Standing Wave Buildup Cavities

REFERENCES.....	59
-----------------	----

LIST OF FIGURES

	Page
FIG. 1. A representation of the index ellipsoid for any crystal with $n_x < n_y < n_z$	14
FIG. 2. (a) The index of refraction profile on the xz plane for a uniaxial crystal. As it can be seen n_x, n_z become equal on the z axis which means z is the optical axis, (b) Indices for a biaxial crystal with the optical axes not along z axis.....	15
FIG. 3. (a). Indices of refraction for positive crystals ($n_e > n_o$), (b) The indices of refraction profiles for negative crystals ($n_o > n_e$).....	16
FIG. 4. A presentation of the principal plane which contains the optical axis and the k vector in the principal coordinate.....	17
FIG. 5. The electric field direction for an extraordinary wave in uniaxial crystals...	17
FIG. 6. The electric field direction for an ordinary wave in uniaxial crystals.....	18
FIG. 7. Index of refraction as a function of θ for (a) the extraordinary, (b) the ordinary beams.....	18
FIG. 8. The phase matching condition for negative uniaxial crystals ($n_o > n_e$).....	29
FIG. 9. The ordinary and the extraordinary electric fields in uniaxial crystals for type I interaction. Vectors x, y and E_o are in orange plane, and k_ω, z and E_e are in the blue plane.....	30
FIG. 10. The k_ω (blue vector refers to the fundamental blue laser light at 486 nm) and $k_{2\omega}$ (violet vector refers to the UV second harmonic laser at 243 nm).....	35
FIG. 11. The walkoff angle between an ordinary an extraordinary wave in a negative uniaxial crystal.....	36
FIG. 12. (a) The ordinary wave vector in an isotropic materials, the ordinary and	

extraordinary propagations in negative (b) and positive (c).....	38
FIG. 13. The walkoff divergence between the ordinary and the extraordinary energy flow and shaping elliptical beams.....	40
FIG. 14. A Gaussian beam focused in a crystal.....	42
FIG. 15. The phase matching condition on the zy plane($\phi = 0$).....	44
FIG. 16. The $h(B)$ factor as a function of B , for $B < 8$	47
FIG. 17. The $h(B)$ factor as a function of B , for $B < 20$	48
FIG. 18. (a) A typical standing wave cavity. (b) A typical ring cavity.....	51
FIG. 19. A buildup cavity with crystal placed inside for SHG and power..... amplification purpose	52
FIG. 20. Plotted β as a function of T_I (at $T_I=0.01$ there is a peak for β).....	56
FIG. 21. Propagation of light at a boundary.....	57
FIG. 22. Brewster cut BBO in a buildup cavity for SHG purpose. Blue lines show fundamental beam of the blue laser at $486.nm$. Violet lines are propagation direction of second harmonic UV laser.....	58

LIST OF TABLES

	Page
TABLE I. Ordinary and extraordinary indices of refraction, birefringence ($\Delta n = n_o - n_e$) at different operating temperatures T and wavelengths λ	20
TABLE II. Theoretical and experimental values of the phase matching angle θ_m (type I, $o + o \rightarrow e$) using BBO. $\lambda_\omega, \lambda_{2\omega}$ are the wavelengths of light for the fundamental and the second harmonic beams.....	28
TABLE III. Calculated d_{eff} for type I phase matching using BBO.....	34
TABLE IV. Calculated walkoff angles for SHG of different frequencies.....	40
TABLE V. Calculated $\theta_m, d_{eff}, \rho, B, h(B)$ and η for SHG of different frequencies using a 10 mm BBO crystal in the room temperature operation.....	50

CHAPTER 1

INTRODUCTION

The laser has produced a significant impact on science and technology. Since immediately after creation of the first laser in 1960 [1], interaction between laser light and materials has been attractive to scientists.

Second harmonic generation (SHG) from a fundamental laser beam was first discovered by Franken et al in 1961 [2]. Franken's group was able to generate radiation of the doubled frequency of a ruby laser by passing its light through a quartz crystal.

Since then, after important discoveries of atomic structures by laser spectroscopic techniques, the monochromatic and coherent laser beams have come to be considered as clean sources of light for laser spectroscopy and material processing [3].

Laser light in the ultra violet (UV) region is very useful for atomic spectroscopy, laser communication, fiber Bragg grating (FBG) writing, and material processing. For example, the two photon excitation of the 1S – 2S interval of hydrogen can be achieved with the 243 *nm* light that we are interested in [4]. High power UV lasers are currently available using rare-gas halide exciter lasers (e.g. XeCl, KrF and ArF). Since these lasers use corrosive gases, they lack frequency stability and pointing stability. They also need regular maintenance and take a lot of space. Scientists prefer compact, maintenancefree, and all solid state lasers for precise experiments.

Today, laser diodes (LD) provide a compact, efficient and reliable source of coherent radiation with very good pointing and frequency stabilities. The use of the LD

is limited only by its wavelength range, which is in the red and infrared part of the spectrum. However, UV laser beams can be generated using nonlinear optical (NLO) properties of nonlinear materials such as beta-barium borate (BBO), lithium triborate (LBO) and periodically poled lithium niobate (PPLN).

Because most experiments in laser spectroscopy can be done by using low power laser beams in the range of $2 \sim 50 \text{ mW}$, harmonic generation from the fundamental frequency of a diode laser represents a reliable alternative to the other laser technologies for UV experiments. Although the low power of the LD makes it more difficult to generate harmonic frequencies due to different losses in the mirrors and crystals, several successful results have been reported [5,6,7]. At the same time, driving a higher frequency laser from a fundamental beam is challenging. At wavelengths less than 300 nm, mirrors and crystals become very absorptive. For example, to do two photon excitation of the 1S- 2S transition in tritium atoms, we need 2 mW of light at 243 nm , but most nonlinear materials are very absorptive at 243 nm . One of the best choices has been BBO crystal due to its higher transparency for $\lambda > 190 \text{ nm}$ than other nonlinear crystals [14]. The following theoretical results suggest that the overall conversion efficiency for SHG from 486 nm with an average power of 50 mW using a BBO crystal would be only 5.9% , using a standing wave buildup cavity .

In this work I will discuss nonlinear optics first. Then I reintroduce one of the most common nonlinear material (BBO) for harmonic generation used currently. The calculation of important physical properties of the experiment is considered.

CHAPTER 2

THEORY OF NONLINEAR OPTICS AND SECOND HARMONIC GENERATION

Linear Polarization

Nonlinear optics is a branch of optics that explains the nonlinear response of atoms and molecules to an optical radiation field. I start with linear optics and then switch to nonlinear optics. This way we can distinguish between nonlinear and linear optics and the response of materials in both cases.

In the classical model of interaction between an electromagnetic field and materials, whenever an electric field is applied on a material, the distance between the electrons and nucleus changes. This effect is called polarization. If the electric field is alternating, the induced polarization alternates too. The frequency of polarization induced on the matter can be considered equal to the frequency of the applied field [8]. Because the distance between electrons and ions is oscillating, this represents a dipole radiation or electromagnetic wave. The dipoles radiate with the same frequency of applied field too. The phase of this oscillation is determined by the restoring force between the electrons and nucleus. Therefore, part of the incident electromagnetic wave is used to produce oscillating dipoles, which radiate a wave with the same frequency but with a different phase.

For calculating linear polarization we use Lorentz's model. In this model we assume that there are N molecules per unit volume with Z electrons each in the matter in which the optical wave has been applied. We also assume that all dipoles reradiate the same fraction of the incident wave. Therefore, the radiation buildup is in the forward

direction and interferes destructively in all other directions [8].

Assume the incident electric field has the form

$$E(x, t) = E(x)e^{i\omega t} = E_0 e^{ikx - i\omega t} \quad (2-1-1)$$

where ω is the frequency of the incident optical wave and E_0 is the maximum amplitude of the alternating wave. To estimate the induced electric dipole moment, we assume the binding force between electron and ion is a restoring force of the form

$$F = -m\omega_0^2 x \quad (2-1-2)$$

where m is the mass of the electron and ω_0 is the binding frequency about equilibrium.

This means that under the action of the external electric field of $E(x, t)$ the electron displaces from its equilibrium by an amount x . Therefore,

$$F = -m\omega_0^2 x = -eE(x, t) \quad (2-1-3)$$

or

$$m\omega_0^2 x = eE(x, t). \quad (2-1-4)$$

In the classical model of electrodynamics, the equation of motion for an electron becomes [12]:

$$m(x'' + \gamma x' + \omega_0^2 x) = -eE(x, t) \quad (2-1-5)$$

where γ is the damping force constant. By replacing $E(x, t)$ with (2-1-1) this becomes

$$m(x'' + \gamma x' + \omega_0^2 x) = -eE(x, t) = -eE(x)e^{-i\omega t} = -E_0 e^{ikx - i\omega t} \quad (2-1-6)$$

and we can write:

$$x'' + \gamma x' + \omega_0^2 x = \frac{-eE_0}{m} e^{ikx - i\omega t}. \quad (2-1-7)$$

If $0 < L \frac{x}{\lambda} \ll 1$, which means the amplitude of oscillation is small enough to permit

evaluation of the electric field at the average position of the electron, x can be written as

$$x = x_0 e^{ikx - i\omega t}. \quad (2-1-8)$$

By plugging (2-1-8) into (2-1-7) we have

$$x_0 (-\omega^2 - i\omega\gamma + \omega_0^2) = \frac{-eE_0}{m}. \quad (2-1-9)$$

The average distance between electron and ion becomes

$$x_0 = \frac{-eE_0}{m(-\omega^2 - i\omega\gamma + \omega_0^2)}. \quad (2-1-10)$$

Therefore, the dipole moment contributed by one electron is

$$p = -ex_0 = \frac{e^2 E_0}{m(-\omega^2 - i\omega\gamma + \omega_0^2)}. \quad (2-1-11)$$

If there are N molecules per unit volume with Z electrons per molecule and each one with its own binding frequency, such that we have f_j electrons per atom with binding frequency ω_j [12] We can write the polarization as

$$P(x, t) = \sum_{j=1}^N p_j = \frac{e^2 N E_0}{m} \sum_{j=1}^N \frac{f_j}{(-\omega_j^2 - i\omega_j\gamma + \omega_0^2)}. \quad (2-1-12)$$

On the other hand polarization can be written as

$$P(x, t) = \epsilon_0 \chi E(x, t). \quad (2-1-13)$$

By comparing (2-1-12) and (2-1-13) the electric susceptibility χ becomes:

$$\chi = \frac{e^2 N}{\epsilon_0 m} \sum_{j=1}^N \frac{f_j}{(-\omega_j^2 - i\omega_j\gamma + \omega_0^2)}. \quad (2-1-14)$$

By knowing the electric susceptibility we can calculate the linear polarization $P(x,t)$. In a crystalline medium the linear susceptibility is a tensor that obeys the symmetry property of the crystal.

Nonlinear Polarization

In the previous section we assumed that polarization is proportional to the electric field. But in real crystals, polarization is caused by an expansion of powers of the applied field such as [10]

$$P(x,t) = \epsilon_0 \chi^{(1)} E(x,t) + \epsilon_0 \chi^{(2)} E^2(x,t) + \epsilon_0 \chi^{(3)} E^3(x,t) + \dots, \quad (2-2-1)$$

where $\chi^{(1)}$ is the linear susceptibility or χ in the last section, $\chi^{(2)}$ is the second order nonlinear susceptibility which is proportional to the electric field quadratically, and $\chi^{(3)}$ is the third order nonlinear susceptibility and so on. $\chi^{(2)}$ and $\chi^{(3)}$ give rise to the second and the third harmonic generation. In this work we are interested in the second harmonic generation interaction. Therefore, we reduce the relation (2-2-1) to the nonlinear second harmonic part

$$P_{NL} = \epsilon_0 \chi^{(2)} E^2(x,t). \quad (2-2-2)$$

Interaction of Two Optical Fields and SHG

In this section we first consider coupling two optical fields with different frequencies. Then we simplify relations for second harmonic generation where both fields have the same frequencies. Assume two optical fields, first:

$$E_i(x_i, t) = E(x_i) e^{-i\omega_1 t} = E_{01} e^{(ikx_i - \omega_1 t)} \quad (2-3-1)$$

where the electric field $E(x, t)$ is a function of x_i (the three orthogonal position coordinates $x_i = x, y, z$ for $i = 1, 2, 3$ respectively) directions with frequency ω_1 , and a second field of:

$$E_j(x_j, t) = E(x_j) e^{-i\omega_2 t} = E_{02} e^{(ikx_j - i\omega_2 t)}. \quad (2-3-2)$$

Similarly, x_j is any of the x , y and z position coordinates and the frequency is ω_2 .

If we apply these two fields to a nonlinear medium, we will observe polarization at a frequency of $\omega_3 = \omega_1 + \omega_2$. Furthermore, (2-2-2) becomes;

$$P_{NL}(x, t) = \epsilon_0 \chi^{(2)} E_i(x, t) E_j(x, t) \quad (2-3-3)$$

or

$$P_{NL}(x, t) = \epsilon_0 \chi_{ijk}^{(2)} E_i(x) e^{-i\omega_1 t} E_j(x) e^{-i\omega_2 t} = \epsilon_0 \chi_{ijk}^{(2)} E_i(x) E_j(x) e^{-i(\omega_1 + \omega_2)t} \quad (1-3-4)$$

Here, $\chi_{ijk}^{(2)}$ is the tensor of the second order electric susceptibility. The frequency of $P_{NL}(x, t)$ is higher than both applied optical fields. If the frequencies of both fields are the same, this represents the second harmonic generation whose polarization has a doubled frequency of each field

$$\omega_3 = 2\omega_1 = 2\omega_2. \quad (2-3-5)$$

Traditionally, nonlinear polarization has been defined by [10]:

$$P_{NL}(x, t) = 2d_{ijk} E_i(x, t) E_j(x, t) \quad (2-3-6)$$

where

$$2d_{ijk} = \epsilon_0 \chi_{ijk}^{(2)} \quad (2-3-7)$$

From now on we will mostly use d_{ijk} as the nonlinear coefficient rather than $\chi_{ijk}^{(2)}$. d_{ijk} is a tensor that can be determined for different crystals depending their chemical structures.

Only crystals with noncentrosymmetric structures can have nonzero elements of d_{ijk} [10].

In a centrosymmetric crystal, by reversing the sign of $E_i(x, t)$ and $E_j(x, t)$ the sign of polarization $P_{NL}(x, t)$ must reverse and not affect the amplitude of polarization.

Therefore, in centrosymmetric crystals we have

$$P_{NL}(x, t) = -2d_{ijk} E_i(x, t) E_j(x, t) = 2d_{ijk} (-E_i(x, t)) (-E_j(x, t)) \quad (2-3-8)$$

which means

$$d_{ijk} = 0. \quad (2-3-9)$$

For a noncentrosymmetric crystal, d_{ijk} is a $3 \times 3 \times 3$ tensor. However, there is no change in the value of the nonlinear coefficient by exchanging i and j in the relation (2-3-6).

Therefore, the tensor d_{ijk} can be reduced to a 6×3 tensor by replacing subscripts ij and ji by contracted indices [9]. Notation of d_{ijk} may be reduced to d_{in} where $n = jk$, or

$d_{i(jk)} = d_{in}$. n can be a number between 1 and 6 corresponding to [10]:

$$n_{xx} = 1, \quad n_{yy} = 2, \quad n_{zz} = 3, \quad n_{yz} = n_{zy} = 4, \quad n_{xz} = n_{zx} = 5, \quad n_{xy} = n_{yx} = 6. \quad (2-3-10)$$

Therefore, d_{in} is reduced to

$$d_{in} = \begin{pmatrix} d_{11} & d_{12} & d_{13} & d_{14} & d_{15} & d_{16} \\ d_{21} & d_{22} & d_{23} & d_{24} & d_{25} & d_{26} \\ d_{31} & d_{32} & d_{33} & d_{34} & d_{35} & d_{36} \end{pmatrix}. \quad (2-3-11)$$

With this definition of the nonlinear coefficient, the polarization becomes:

$$\begin{pmatrix} P_x \\ P_y \\ P_z \end{pmatrix} = \begin{pmatrix} d_{11} & d_{12} & d_{13} & d_{14} & d_{15} & d_{16} \\ d_{21} & d_{22} & d_{23} & d_{24} & d_{25} & d_{26} \\ d_{31} & d_{32} & d_{33} & d_{34} & d_{35} & d_{36} \end{pmatrix} \times \begin{pmatrix} E_x E_x \\ E_y E_y \\ E_z E_z \\ 2E_y E_z \\ 2E_z E_x \\ 2E_x E_y \end{pmatrix} \quad (2-3-12)$$

The polarization components the in three directions of x, y and z become:

$$\begin{aligned} P_x &= d_{11}(E_x E_x) + d_{12}(E_y E_y) + d_{13}(E_z E_z) + 2d_{14}(E_y E_z) + 2d_{15}(E_z E_x) + 2d_{16}(E_x E_y) \\ P_y &= d_{21}(E_x E_x) + d_{22}(E_y E_y) + d_{23}(E_z E_z) + 2d_{24}(E_y E_z) + 2d_{25}(E_z E_x) + 2d_{26}(E_x E_y) \\ P_z &= d_{31}(E_x E_x) + d_{32}(E_y E_y) + d_{33}(E_z E_z) + 2d_{34}(E_y E_z) + 2d_{35}(E_z E_x) + 2d_{36}(E_x E_y). \end{aligned} \quad (2-3-13)$$

As we can see, the factor of 2 in Eq. (2-3-6) applies for the interaction of two fields in two different directions such as E_x and E_y , where coupling is possible in two different way: $E_x E_y$ or $E_y E_x$. But in the interaction of two fields in the same direction there is only one possible way such as $E_x E_x$. Thus the factor 2 is not applicable.

Depending on what coefficients from d_{11} to d_{36} are nonvanishing we can have various coupling possibilities. For example, the BBO crystal with point group 3m- C_{3c} (symmetry with respect to x direction) has the following d_{in} tensor [10]:

$$d_{in} = \begin{pmatrix} 0 & 0 & 0 & 0 & d_{15} & -d_{22} \\ -d_{22} & d_{22} & 0 & d_{15} & 0 & 0 \\ d_{31} & d_{31} & d_{32} & 0 & 0 & 0 \end{pmatrix}. \quad (2-3-14)$$

This means

$$d_{11} = d_{12} = d_{13} = d_{14} = d_{23} = d_{25} = d_{26} = d_{34} = d_{35} = d_{30} = 0. \quad (2-3-15)$$

The nonvanishing coefficients are

$$d_{15}, d_{16}, d_{21}, d_{22}, d_{24}, d_{31}, d_{32}, d_{33}. \quad (2-3-16)$$

These nonvanishing constants can be related to each other according to the crystal symmetry. For a BBO crystal nonvanishing coefficients are related as

$$d_{16} = -d_{22}, \quad d_{21} = -d_{22}, \quad d_{24} = -d_{15}. \quad (2-3-17)$$

Therefore, the possible coupling interactions using a BBO crystal are

$$P_x = 2d_{15}(E_z E_x) - 2d_{22}(E_x E_y) \quad (2-3-18)$$

$$P_y = -d_{22}(E_x E_x) + d_{22}(E_y E_y) - 2d_{15}(E_y E_z) \quad (2-3-19)$$

$$P_z = d_{31}(E_x E_x) + d_{32}(E_y E_y) + d_{33}(E_z E_z). \quad (2-3-20)$$

Since the z axis is always considered as the optic axis, this means that the electric field in the z direction is equal to zero. Therefore the set of equations above become:

$$E_z = 0$$

$$P_x = -2d_{22}(E_x E_y) \quad (2-3-21)$$

$$P_y = -d_{22}(E_x E_x) + d_{22}(E_y E_y) \quad (2-3-22)$$

$$P_z = d_{31}(E_x E_x) + d_{32}(E_y E_y). \quad (2-3-23)$$

CHAPTER 3

OPTICS OF UNIAXIAL CRYSTALS

Because we are interested in using a BBO crystal for second harmonic generation of the laser light at 486 nm , we focus on the optical properties of uniaxial crystals. BBO is a negative, uniaxial and anisotropic crystal with a trigonal system (point group $3m-C_{3v}$). In this chapter I explain wave propagation and the phase matching condition in uniaxial crystals. I also define and calculate important parameters such as the phase matching angle θ_m , the walkoff angle between the fundamental and the second harmonic energy flow directions ρ , and the effective nonlinear coefficient d_{eff} for SHG of light at 486 nm . Finally the single pass conversion efficiency η using BBO will be calculated.

Light Propagation in an Anisotropic Medium

In most nonlinear crystals, optical properties depend on the propagation direction and also the polarization direction [10]. The difference between isotropic and anisotropic lies in the directions of propagation and polarization of light. In isotropic materials, the polarization direction is always parallel to the electric field of optical wave. However, in an anisotropic crystal the polarization direction can be in a different direction from the applied electric field. The dielectric response of crystals to an external field can be written as

$$D_x = \epsilon_{11}E_x + \epsilon_{12}E_y + \epsilon_{13}E_z \quad (3-1-1)$$

$$D_y = \epsilon_{21}E_x + \epsilon_{22}E_y + \epsilon_{23}E_z \quad (3-1-2)$$

$$D_z = \epsilon_{31}E_x + \epsilon_{32}E_y + \epsilon_{33}E_z \quad (3-1-3)$$

where ϵ_{ij} is the dielectric permeability tensor. ϵ_{ij} is defined as

$$\epsilon_{ij} = \epsilon_0 (1 + \chi_{ij}) \quad (3-1-4)$$

where χ_{ij} is the electric susceptibility, discussed in last the chapter, and ϵ_0 is the air dielectric constant. Therefore, the equations (3-1-1 \rightarrow 3) can be written as

$$D_i = \epsilon_{ij} E_j \quad (3-1-5)$$

where i, j can have the values of 1, 2 and 3. They stand for $x = 1, y = 2, z = 3$. With this definition, the energy density of a stored electric field in an anisotropic crystal like any other medium is:

$$U = \frac{1}{2} ED = \frac{1}{2} E_i \epsilon_{ij} E_j \quad (3-1-6)$$

where ϵ_{ij} in the principal coordinate system can be written as [10]

$$\epsilon_{ij} = \begin{pmatrix} \epsilon_{11} & 0 & 0 \\ 0 & \epsilon_{22} & 0 \\ 0 & 0 & \epsilon_{33} \end{pmatrix} = \begin{pmatrix} \epsilon_x & 0 & 0 \\ 0 & \epsilon_y & 0 \\ 0 & 0 & \epsilon_z \end{pmatrix}. \quad (3-1-7)$$

In the anisotropic crystals, the phase velocity of light depends on both the polarization state and the propagation direction [10]. Anisotropic properties causes the variation of polarization state as light propagates through a crystal. The surface of constant energy density in three dimension (3-1-6) can be written as

$$2U = ED = E_i \epsilon_{ij} E_j = E_x \epsilon_x E_x + E_y \epsilon_y E_y + E_z \epsilon_z E_z. \quad (3-1-8)$$

By replacing E_i with $\frac{D_i}{\epsilon_i}$, the relation above becomes

$$2U = \frac{D_x^2}{\epsilon_x} + \frac{D_y^2}{\epsilon_y} + \frac{D_z^2}{\epsilon_z}, \quad (3-1-9)$$

where ϵ_x , ϵ_y and ϵ_z are the principal dielectric constants. The phase velocity v_{ph} of the wave is [12]

$$v_{ph} = \frac{c}{n} = \frac{\omega}{k} = \frac{1}{\sqrt{\mu\epsilon}}, \text{ with } n = \sqrt{\frac{\mu\epsilon}{\mu_0\epsilon_0}}, \quad (3-1-10)$$

where c is the speed of light, n is the index of refraction, ω is the angular frequency of the light, and k is wave number. Because nonlinear crystals are nonmagnetic materials, $\mu = \mu_0 = 1$ and $\epsilon_0 = 1$, and the indices of refraction in three the directions x, y and z become

$$n_x = \sqrt{\epsilon_x}, \quad n_y = \sqrt{\epsilon_y}, \quad n_z = \sqrt{\epsilon_z}; \quad (3-1-11)$$

these are n_x , n_y , n_z are the principal indices of refraction. The principal axes x, y and z are defined by

$$x^2 = \frac{D_x^2}{2U}, \quad y^2 = \frac{D_y^2}{2U}, \quad z^2 = \frac{D_z^2}{2U}. \quad (3-1-12)$$

By plugging (3-1-11) and (3-1-12) into the relation (3-1-9), we can write

$$\frac{x^2}{n_x^2} + \frac{y^2}{n_y^2} + \frac{z^2}{n_z^2} = 1. \quad (3-1-13)$$

This is the equation of an ellipsoid with the lengths $2n_x$, $2n_y$ and $2n_z$ in the directions of the principal axes for any crystal including biaxial and uniaxial. This relation is called the index ellipsoid equation. The surface of the index ellipsoid provides useful information about optical wave propagation in anisotropic crystals. If $n_x > n_y > n_z$, the crystal is called negative biaxial. On the other hand, a crystal with $n_x < n_y < n_z$ is called

positive biaxial. Fig. 1 is an example of the index ellipsoid for a positive crystal.

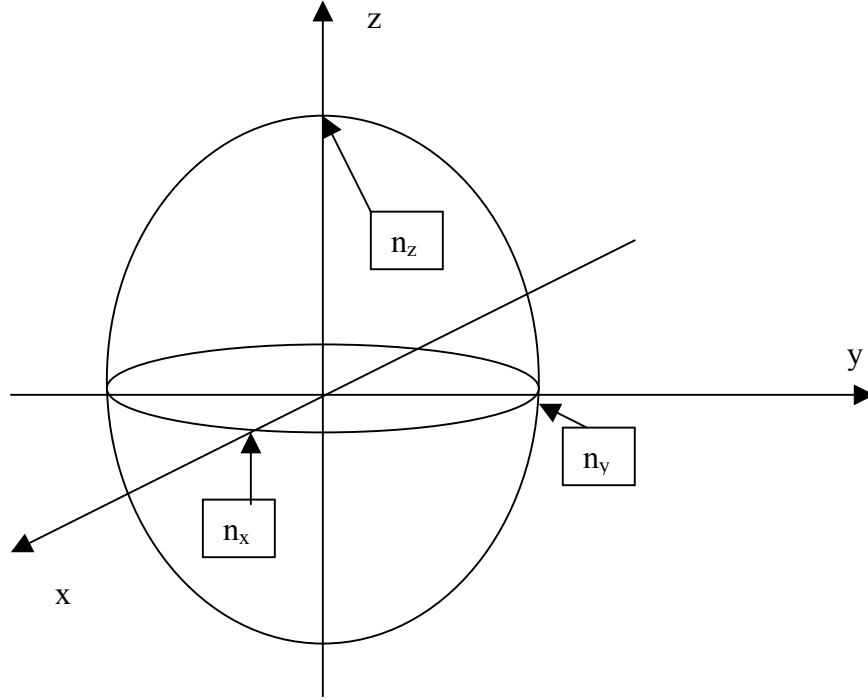


FIG. 1. A representation of the index ellipsoid for any crystal with $n_x < n_y < n_z$.

When n_x , n_y and n_z have different values, the crystal has two optical axes [10].

In this case, the crystal is called biaxial. Uniaxial crystals are special case of biaxial crystals which the indices of refraction along two principal axes become the same and constant for any direction with respect to optical axis. This means that there is no distinction between indices of refraction n_y and n_x in two directions, we can write

$$n_x^2 = n_y^2 = \frac{\epsilon_x}{\epsilon_0} = \frac{\epsilon_y}{\epsilon_0}. \quad (3-1-14)$$

In this case, there would be only one optical axis, which is the z axis. Fig. 2. shows the index profiles and optic axes for biaxial and uniaxial crystals.

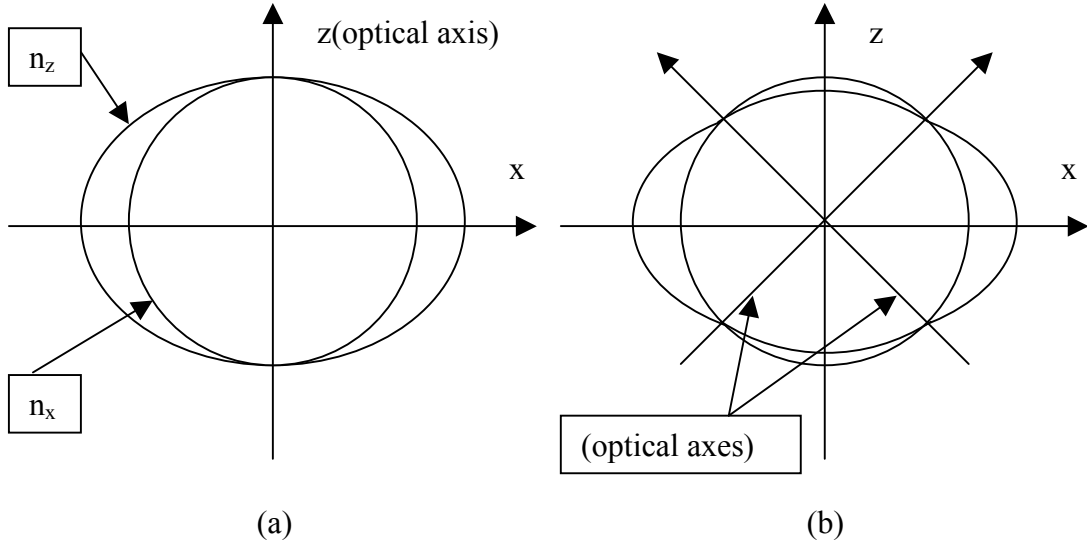


FIG. 2. (a) The index of refraction profile on the xz plane for a uniaxial crystal. As can be seen n_x & n_z become equal on the z axis which means z is the optical axis.
 (b) Indices for biaxial crystal with the optical axes not along z axis.

For uniaxial crystals, n_x and n_y are equal and called the ordinary index of refraction:

$$n_o = n_x = n_y \quad (3-1-15)$$

On the other hand, n_z is called the extraordinary index of refraction:

$$n_e = n_z \quad (3-1-16)$$

Uniaxial crystals with $n_o > n_e$ are called negative. If $n_e > n_o$, the crystal is called positive. Intersections of normal surfaces with the xz plane for positive and negative uniaxial crystals are shown in the Fig. 3. (a),(b).

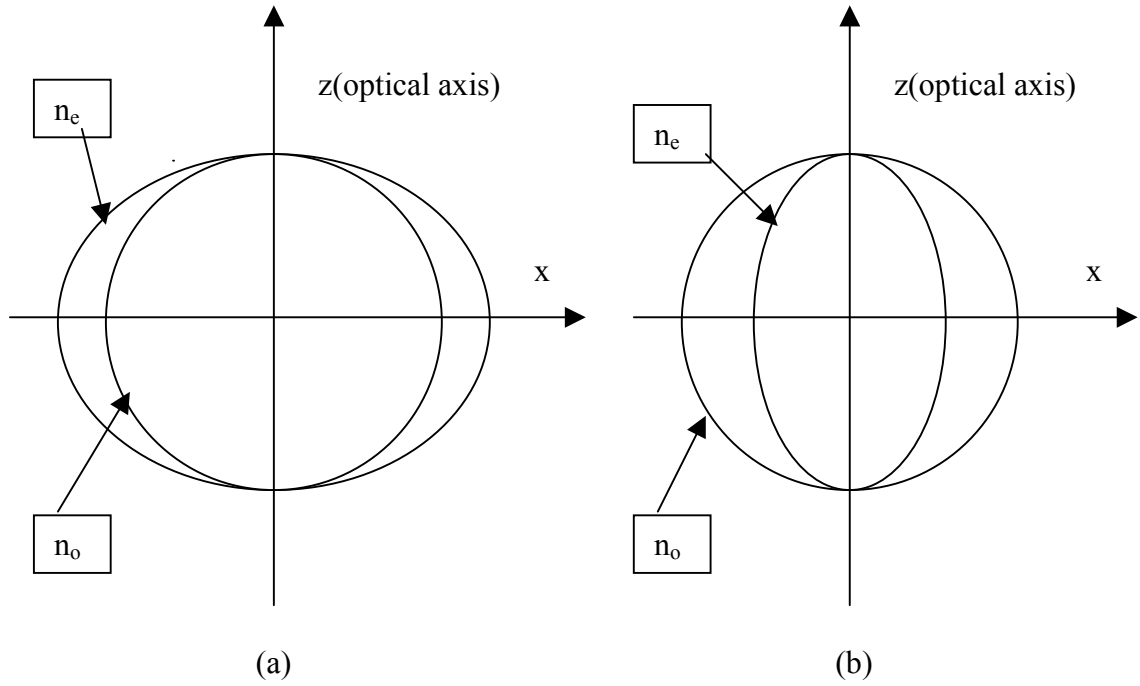


FIG. 3. (a) Indices of refraction for positive crystals ($n_e > n_o$) and (b) The indices of refraction profiles for negative crystals ($n_o > n_e$).

Propagation of Light in Uniaxial Crystals

As we mentioned before, the z direction is always the optical axis for uniaxial crystals. The plane that contains the optical axis and the wave vector k of the light is called the principal plane [13]. FIG. 4. shows the optical axis z , light propagation direction k and the principal plane for a uniaxial crystal.

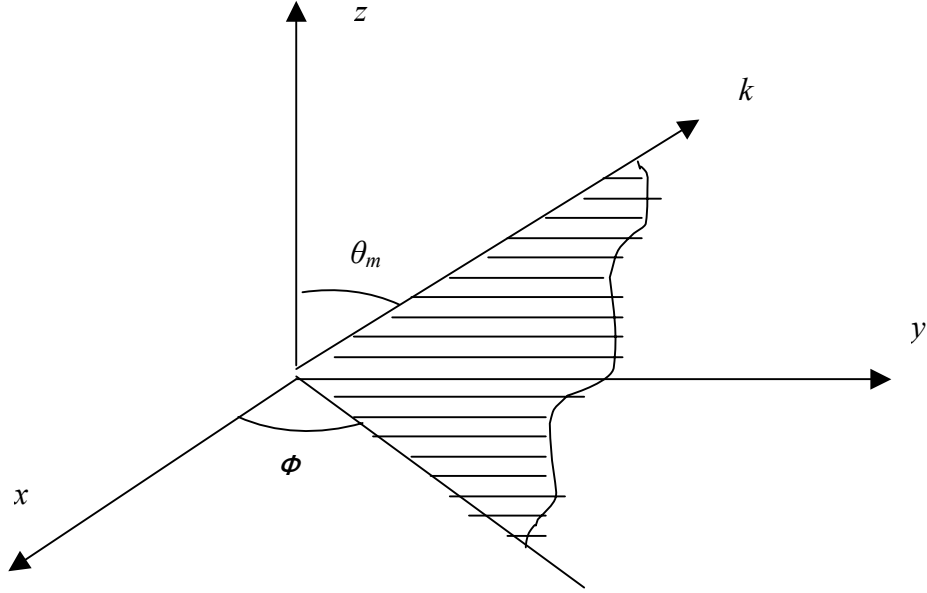


FIG. 4. The principal plane which contains the optical axis and the k vector in the principal coordinate system.

For the extraordinary light beam the polarization direction is always in the principal plane, as Fig. 5. shows.

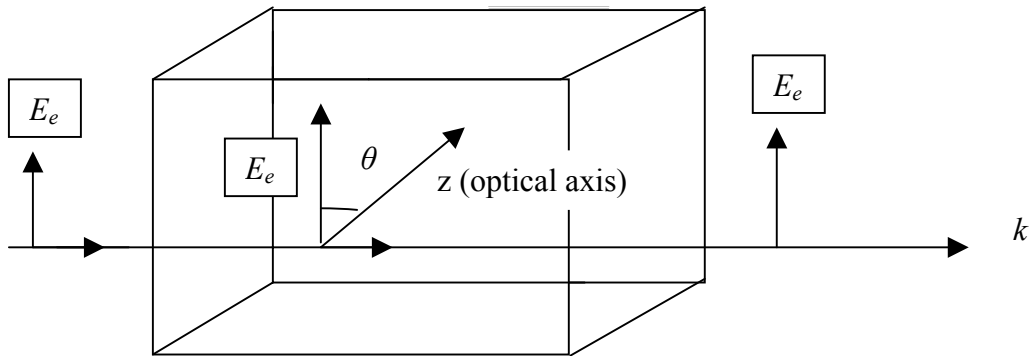


FIG. 5. The electric field direction for an extraordinary wave in uniaxial crystals.

On the other hand, the polarization direction for the ordinary light lies on the

plane normal to the principal plane, Fig. 6.

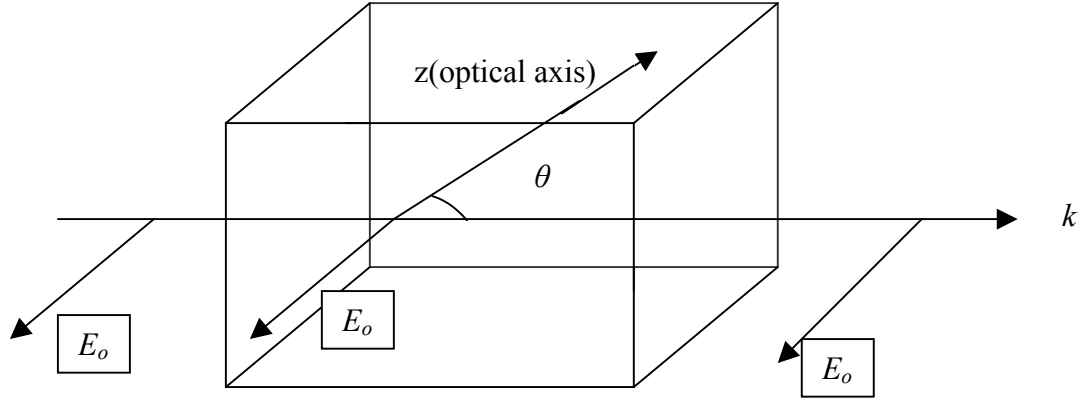


FIG. 6. The electric field direction for an ordinary wave in uniaxial crystals.

The index of refraction for the ordinary light doesn't depend on the propagation direction, but for the extraordinary beam it does [13]. That is, the index of refraction for the ordinary beam does not depend on the angle θ with respect to the optical axis z . But for an extraordinary beam the index of refraction varies by changing the direction of propagation with respect to the optical axis. Indices of refraction of the extraordinary and the ordinary light as a function θ are shown in the figure below.

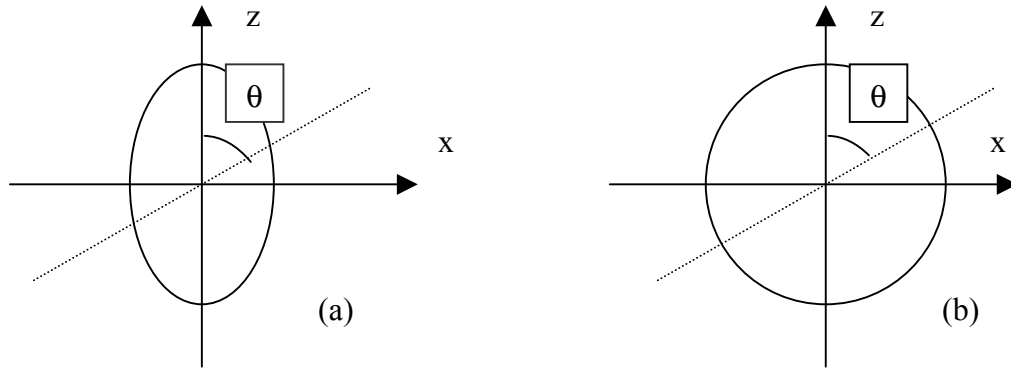


FIG. 7. Index of refraction as a function of θ for (a) the extraordinary and (b) the ordinary beams

The extraordinary index of refraction can vary as a function of θ for a fixed frequency ω , but the ordinary index of refraction is constant:

$$n_{o\omega}(\theta) = n_{o\omega}, \quad (3-2-1)$$

$$\frac{1}{n_{e(\omega)}^2(\theta)} = \frac{\cos^2(\theta)}{n_{o(\omega)}^2} + \frac{\sin^2(\theta)}{n_{e(\omega)}^2}. \quad (3-2-2)$$

As was mentioned before, for an anisotropic crystal the index of refraction depends on light propagation as well as polarization direction. The difference between the value of the indices of refraction for ordinary light (n_o) and extraordinary light (n_e) is called the birefringence, Δn :

$$\Delta n = n_o - n_e \quad (3-2-3)$$

Along the optic axis, Δn becomes zero. Δn increases in moving from the optical axis (z) to any x or y directions and it reaches to its maximum on the xy plane.

Indices of refraction for both the ordinary and the extraordinary light are functions of the frequency of light and the operating temperature of the crystal. Conventionally, the indices of refraction for ordinary and extraordinary beams are shown in the Sellmeier form. For example, BBO has the following Sellmeier relations for n_o and n_e as a function wavelength $\lambda(\mu m)$ at room temperature [14]:

$$n_e^2 = 2.3730 + \frac{0.0128}{\lambda^2 - 0.0156} - 0.0044\lambda^2, \quad \text{for BBO} \quad (3-3-4)$$

$$n_o^2 = 2.7405 + \frac{0.0184}{\lambda^2 - 0.0179} - 0.0155\lambda^2. \quad \text{for BBO} \quad (3-3-5)$$

BBO is a negative uniaxial crystal, with $n_o > n_e$. The indices of refraction for BBO

change very slightly with temperature. n_o and n_e as functions of temperature have been represented by [14]

$$\frac{dn_o(\lambda)}{dT} = \frac{-16.6 \times 10^{-6}}{^{\circ}C} \quad \text{for BBO} \quad (3-2-6)$$

$$\frac{dn_e(\lambda)}{dT} = \frac{-9.3 \times 10^{-6}}{^{\circ}C} \quad \text{for BBO} \quad (3-2-7)$$

The indices of refraction change very slightly with temperature and precision temperature tuning is one of the techniques for improving the phase matching condition and in a nonlinear SHG process. Table I shows the values of indices of refraction of BBO at different wavelengths (including 486 *nm* and 243 *nm* that we are interested in) for the ordinary and the extraordinary beams at room temperature (25°C) and 75°C.

TABLE I. The ordinary and the extraordinary indices of refraction, birefringence ($\Delta n = n_o - n_e$) at different operating temperatures T and wavelengths λ .

	$T = 25^{\circ}C$			$T = 75^{\circ}C$		
λ (wavelength)	n_o	n_e	Δn	n_o	n_e	Δn
243 <i>nm</i>	1.6872	1.5643	0.1229	1.6858	1.5635	0.1223
486 <i>nm</i>	1.6796	1.5588	0.1208	1.6782	1.5581	0.1201
532 <i>nm</i>	1.6749	1.5555	0.1194	1.6735	1.5547	0.1188
1064 <i>nm</i>	1.6551	1.5425	0.1126	1.6537	1.5418	0.1119

A quick look at the values in the Table I shows that for BBO the ordinary and the extraordinary indices of refraction as well as Δn decrease with increasing wavelength. It

also can be seen that by increasing the temperature the values of n_o, n_e and birefringence Δn decrease for a corresponding wavelength.

Phase Matching Conditions for SHG in Uniaxial Crystals

The phase matching angle is the angle with respect to the optical axis at which the fundamental beam has to propagate inside the crystal principal axis configuration to optimize SHG. There are two angles that we mention throughout this chapter, θ_m (the phase matching angle) and ϕ , which is the azimuthal angle with respect to the x or y direction. The angle ϕ determines an effective k vector direction in the crystal. To calculate the phase matching angle θ_m , we need to start with Maxwell's equations [12]:

$$\nabla \times H = \frac{\partial D}{\partial t} + J \quad (3-3-1)$$

$$\nabla \times E = -\frac{\partial B}{\partial t} \quad (3-3-2)$$

$$H = \frac{B}{\mu} \quad (3-3-3)$$

$$J = \sigma E \quad (3-3-4)$$

$$D = \epsilon E + P_{NL} \quad (3-3-5)$$

$$\epsilon = \epsilon_o (1 + \chi) . \quad (3-3-6)$$

Here P_{NL} is the nonlinear polarization, discussed and defined by (2-2-2). Taking the curl of both sides of Eq. (3-3-2), we have

$$\nabla \times (\nabla \times E) = \nabla \times \left(-\frac{\partial B}{\partial t} \right) . \quad (3-3-7)$$

Nonlinear crystals such as BBO are nonmagnetic materials ($\mu = \mu_0$). Using

$H = \frac{B}{\mu}$, we can write

$$\nabla \times (\nabla \times E) = \left(-\frac{\partial}{\partial t}\right)(\nabla \times \mu_o H). \quad (3-3-8)$$

If

$$\nabla \times (\nabla \times E) = \nabla(\nabla \cdot E) - \nabla^2 E \quad \text{and} \quad \nabla \cdot E = 0, \quad (3-3-9)$$

Eq. (3-3-7) becomes:

$$-\nabla^2 E = -\mu_o \frac{\partial}{\partial t}(\nabla \times H). \quad (3-3-10)$$

By replacing $\nabla \times H$ from (3-3-1), we can show:

$$-\nabla^2 E = -\mu_o \frac{\partial}{\partial t} \left(\frac{\partial D}{\partial t} + J \right), \quad (3-3-11)$$

or

$$\nabla^2 E = \mu_o \left(\frac{\partial^2 D}{\partial t^2} + \frac{\partial J}{\partial t} \right). \quad (3-3-12)$$

By substituting D from (3-3-5) and J from (3-3-4), (3-3-12) becomes:

$$\nabla^2 E = \mu_o \left(\frac{\partial^2 (\epsilon E + P_{NL})}{\partial t^2} + \frac{\partial (\sigma E)}{\partial t} \right). \quad (3-3-13)$$

Finally, it can be reduced to:

$$\nabla^2 E - \mu_o \frac{\partial^2 P_{NL}}{\partial t^2} - \mu_o \epsilon \frac{\partial^2 E}{\partial t^2} - \sigma \mu_o \frac{\partial E}{\partial t} = 0. \quad (3-3-14)$$

This equation describes the electric field E generated by the polarization P_{NL} . The fields in Eq. (3-3-14) are instantaneous fields [9].

As was mentioned before, z is the optical axis; therefore, the plane wave propagation direction in the z direction requires:

$$\frac{\partial E}{\partial x} = \frac{\partial E}{\partial y} = 0 \quad (3-3-15)$$

Solutions for equation (3-3-14) can be the real part of oscillating fields. Three solutions for (3-3-14) can be fields of $E_1(z, t)$, $E_2(z, t)$ and $E_3(z, t)$ with

$$E_1(z, t) = \text{Re}\{E_1(\omega_1, z)e^{i(\omega_1 t - k_1 z)}\} = \frac{1}{2}\{E_1(\omega_1, z)e^{i(\omega_1 t - k_1 z)}\} \quad (3-3-16)$$

$$E_2(z, t) = \text{Re}\{E_2(\omega_2, z)e^{i(\omega_2 t - k_2 z)}\} = \frac{1}{2}\{E_2(\omega_2, z)e^{i(\omega_2 t - k_2 z)}\} \quad (3-3-17)$$

$$E_3(z, t) = \text{Re}\{E_3(\omega_3, z)e^{i(\omega_3 t - k_3 z)}\} = \frac{1}{2}\{E_3(\omega_3, z)e^{i(\omega_3 t - k_3 z)}\}. \quad (3-3-18)$$

We recall Eq. (2-3-6) and replace d_{ijk} by d_{eff} which is called the effective nonlinear coefficient. d_{eff} depends on crystal symmetry and is a function of the phase matching angle θ_m and the azimuthal angle ϕ . d_{ijk} and d_{in} values were discussed on page 8. d_{eff} will be discussed in the next section.

Now, the polarization (with frequency ω_3) of two coupled waves with frequencies equal to ω_1 , ω_2 can be written as

$$P_{NL}(\omega_3, z, t) = 2d_{eff}E_1(z, t)E_2(z, t). \quad (3-3-19)$$

If the interacting fields $E_1(\omega_1, z, t)$ and $E_2(\omega_2, z, t)$ have the same frequencies $\omega = \omega_1 = \omega_2$, and the field $E_3(\omega_3, z, t)$ has frequency of $2\omega = 2\omega_1 = 2\omega_2 = \omega_3$, the interaction represents the second harmonic generation polarization. Polarizations of the fundamental wave at ω and the second harmonic at 2ω can be calculated by plugging (3-3-16), (3-3-17) and (3-3-18) into (3-3-19):

$$P_{NL}(\omega, z, t) = 2d_{eff}E_3(2\omega, t)E_1^*(\omega, t)e^{i(k_{2\omega} - 2k_\omega)z} \quad (3-3-20)$$

$$P_{NL}(2\omega, z, t) = d_{eff} E_1^*(\omega, t) E_2(\omega, t) e^{i(2k_\omega - k_{2\omega}) \cdot z} \quad (3-3-21)$$

where $E_1^*(\omega, t)$ is the complex conjugate of $E_1(\omega, t)$, and k_ω and $k_{2\omega}$ are wave numbers for the fundamental and the second harmonic beams. In order to have the fundamental and the second harmonic polarizations in phase, we have to impose the condition of

$$k_{2\omega} - 2k_\omega = 2k_\omega - k_{2\omega}. \quad (3-3-22)$$

This means

$$k_{2\omega} = 2k_\omega \quad (3-3-23)$$

The equation above is the phase matching condition for effective nonlinear second harmonic generation. We would like to translate this phase matching condition into the information containing indices of refraction for the ordinary and the extraordinary beams.

To do so, we can define k_ω and $k_{2\omega}$ as

$$k_\omega = \omega \sqrt{\epsilon \mu} n_\omega, \quad (3-3-24)$$

$$k_{2\omega} = 2\omega \sqrt{\epsilon \mu} n_{2\omega}. \quad (3-3-25)$$

Therefore, condition (3-3-23) becomes:

$$2k_\omega = k_{2\omega} = 2\omega \sqrt{\epsilon \mu} n_\omega = 2\omega \sqrt{\epsilon \mu} n_{2\omega} \quad (3-3-26)$$

By simplifying (3-3-26) we can define the phase matching condition in the new form

$$n_{2\omega} = n_\omega. \quad (3-3-27)$$

This means for having the second harmonic generation, the indices of refraction for the fundamental and the second harmonic waves must be equal.

Two Different Types of Phase Matching in Negative Uniaxial Crystals

In the previous section I found a general relationship for the phase matching condition. If two fundamental interacting wave have the same polarization, this is called type I phase matching [13]. For example, in negative crystals two ordinary waves with the same direction of polarization can generate an extraordinary second harmonic wave (type I). This condition can be symbolized as

$$\begin{aligned} o + o &\rightarrow e, \\ k_{ow} + k_{ow} &= k_{e(2\omega)}(\theta). \end{aligned} \quad (3-4-1)$$

However, if two interacting fundamental waves have different polarizations such as one ordinary wave and the other one extraordinary, the interaction is called type II phase matching. For negative uniaxial crystals, there are two possibilities for type II phase matching, first,

$$\begin{aligned} o + e &\rightarrow e \\ k_{ow} + k_{ew}(\theta) &= k_{e(2\omega)}(\theta), \end{aligned} \quad (3-4-2)$$

and second

$$\begin{aligned} e + o &\rightarrow e \\ k_{ew}(\theta) + k_{ow} &= k_{e(2\omega)}(\theta). \end{aligned} \quad (3-4-3)$$

In this work we are interested in $o + o \rightarrow e$ (type I) interaction, which means two ordinary waves at 486 nm wavelength interact and result in an extraordinary second harmonic wave with 243 nm wavelength. Applying the condition (3-3-27), it requires that the ordinary index of refraction at 486 nm must be equal to the extraordinary index of

refraction at 243 nm,

$$n_{o(\omega)} = n_{e(2\omega)}(\theta_m), \quad (3-4-4)$$

to have optimum phase matching. Recalling equation (3-2-2) and replacing θ , which is an arbitrary angle, with the phase matching angle θ_m , it becomes:

$$\frac{1}{n_{e(2\omega)}^2(\theta_m)} = \frac{\cos^2(\theta_m)}{n_{o(2\omega)}^2} + \frac{\sin^2(\theta_m)}{n_{e(2\omega)}^2}. \quad (3-4-5)$$

By plugging $n_{o(\omega)} = n_{e(2\omega)}(\theta_m)$ into the above equation, I can rewrite it as

$$\frac{1}{n_{o(\omega)}^2} = \frac{\cos^2(\theta_m)}{n_{o(2\omega)}^2} + \frac{\sin^2(\theta_m)}{n_{e(2\omega)}^2} \quad (3-4-6)$$

Using the relation $\cos^2(\theta_m) = 1 - \sin^2(\theta_m)$ and solving (3-4-5) for θ_m , the phase matching angle becomes:

$$\sin^2(\theta_m) = \frac{n_{o(\omega)}^{-2} - n_{o(2\omega)}^{-2}}{n_{e(2\omega)}^{-2} - n_{o(2\omega)}^{-2}} \quad (3-4-7)$$

This is the equation that determines the phase matching angle for a type I interaction ($o + o \rightarrow e$) for second harmonic generation using a negative uniaxial crystal like BBO. This situation can be explained by the figure below.

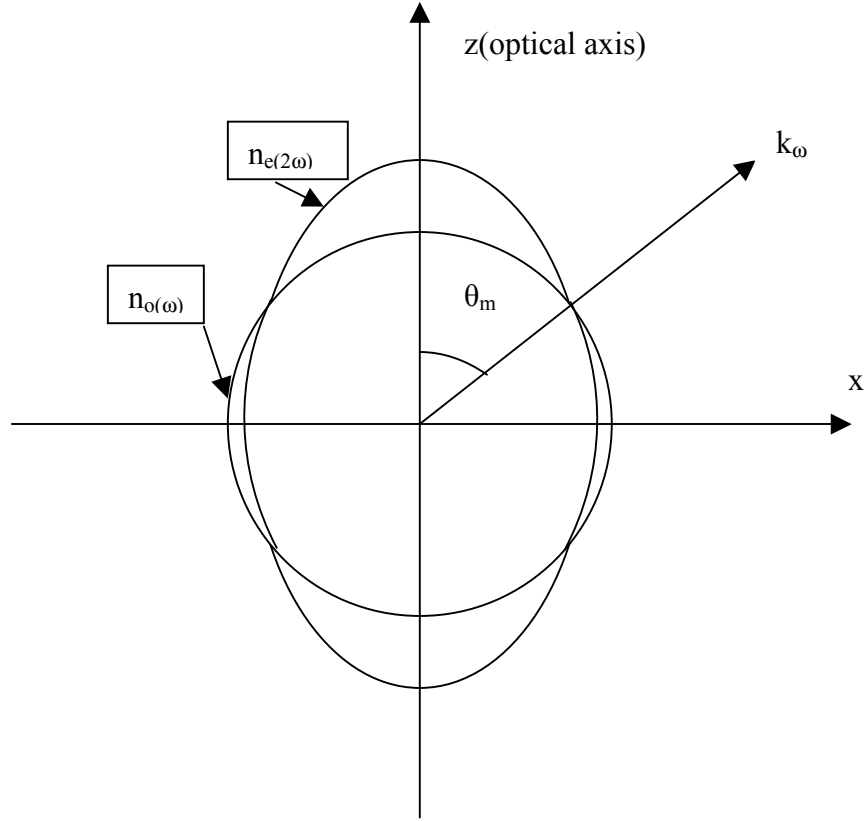


FIG. 8. The phase matching condition for negative uniaxial crystals ($n_o > n_e$)

We are going to generate a UV laser beam at 243 nm by the second harmonic generation (type I phase matching) of a blue laser at 486 nm . Using the values in Table I, we can calculate θ_m for our application using a BBO crystal at room temperature:

$$n_{o(\omega)} = 1.6797 \quad n_{e(\omega)} = 1.5588 \quad (\lambda_{\omega} = 486 \text{ nm})$$

$$n_{o(2\omega)} = 1.6872 \quad n_{e(2\omega)} = 1.5643 \quad (\lambda_{2\omega} = 243 \text{ nm})$$

$$\sin^2(\theta_m) = \frac{n_{o(\omega)}^{-2} - n_{o(2\omega)}^{-2}}{n_{e(2\omega)}^{-2} - n_{o(2\omega)}^{-2}} = \frac{(1.6797)^{-2} - (1.6872)^{-2}}{(1.5643)^{-2} - (1.6872)^{-2}} = 0.6655 \quad (3-4-8)$$

$$\sin(\theta_m) = 0.8158;$$

$$\theta_m = 54.667^\circ. \quad (3-4-9)$$

TABLE II. Theoretical and experimental values of the phase matching angle θ_m (type I , $o + o \rightarrow e$) using BBO. $\lambda_\omega, \lambda_{2\omega}$ are the wavelengths of light for the fundamental and the second harmonic beams respectfully.

$\lambda_\omega \Rightarrow \lambda_{2\omega}$	θ_m (Theoretical)	θ_m (Experimental)	Reference
410 nm \Rightarrow 205 nm	85.535°	90°	[18]
486 nm \Rightarrow 243 nm	54.667°	--	--
488 nm \Rightarrow 244 nm	54.288°	54.5°	[19]
532 nm \Rightarrow 266 nm	47.529°	47.3°	[14]
710 nm \Rightarrow 355 nm	32.913°	32.9°	[20]
1064 nm \Rightarrow 532 nm	22.880°	22.7°	[21]

The Effective Nonlinear Coefficient

Recalling Eq. (3-3-19), to calculate the polarization of the second harmonic wave, we need to know the electric fields components for the ordinary and the extraordinary waves for type I and II interactions. Let's start with electric field directions in the principal coordinates. The general equation

$$P_{NL}(2\omega, z, t) = 2d_{eff}E_1(\omega, z, t)E_2(\omega, z, t) \quad (3-5-1)$$

does not contain information about the effective magnitude of electric fields. This was the reason for replacing d_{ijk} by d_{eff} . The nonlinear coefficient d_{eff} translates a general polarization $P_{NL}(2\omega, z, t)$ to an intended interaction in the principal coordinates. For example, we are interested in an $o + o \rightarrow e$ interaction. For calculating the polarization of the second harmonic wave, we need to know the electric field magnitude of the ordinary wave according to crystal symmetry. Fig. 9 shows the directions of electric fields for an ordinary and extraordinary waves in negative uniaxial crystals. By looking at Fig. 9, we can show that the components of the electric fields for the ordinary and the extraordinary waves are:

$$\begin{aligned} E_{ox} &= |E_o| \sin \phi & E_{ex} &= |E_o| (-\cos \phi \cos \theta_m) \\ E_{oy} &= |E_o| (-\cos \phi) & E_{ey} &= |E_o| (-\sin \phi \cos \theta_m) \\ E_{oz} &= 0 & E_{ez} &= |E_o| (\sin \theta_m) \end{aligned} \quad (3-5-2)$$

Here E_{ox} , E_{oy} , E_{oz} are the electric field components for the ordinary beam in the x, y, z principal axes. E_{ex} , E_{ey} and E_{ez} are the components of the electric field for an

extraordinary wave on the principal axes. $|E_o|$ is the magnitude of the ordinary electric field.

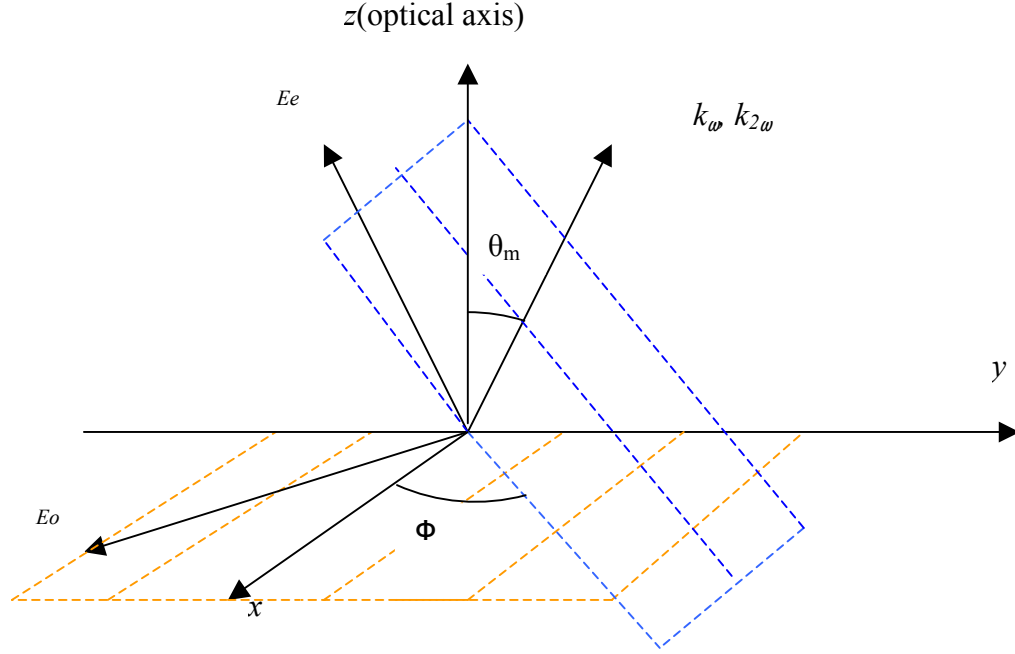


FIG. 9. The ordinary and the extraordinary electric fields in uniaxial crystals for type I interaction. x , y and E_o are in the orange plane, and k_ω , z and E_e are in the blue plane.

Using these field components, we can write a general relation for the polarization second harmonic wave. For type I interaction ($o + o \rightarrow e$) using a uniaxial crystal, relation (3-5-1) becomes:

$$|P_e| = (2 - \delta_{jk}) d_{ijk} A_j A_k B_i |E_o|^2. \quad (3-5-3)$$

where

$$A_j = \begin{vmatrix} \sin \phi \\ -\cos \phi \\ 0 \end{vmatrix} \quad j = 1, 2, 3 \text{ for } x, y, z \text{ directions}$$

$$B_j = \begin{vmatrix} -\cos\phi\cos\theta_m \\ -\sin\phi\cos\theta_m \\ \sin\theta_m \end{vmatrix} \quad j = 1,2,3 \text{ for } x,y,z \text{ directions}$$

By comparing (3-5-2) to the general form of

$$P_{eNL}(2\omega) = d_{eff} E_o(\omega) E_o(\omega) \quad (3-5-4)$$

for an $o + o \rightarrow e$ where $P_{eNL}(2\omega)$ is the second harmonic polarization, d_{eff} can be written as:

$$d_{eff} = (2 - \delta_{jk}) d_{ijk} A_j A_k B_i. \quad (3-5-5)$$

Similarly, for type II interaction ($o + e \rightarrow e$ or $e + o \rightarrow e$) in the negative crystals we have:

$$|P_e| = (2 - \delta_{jk}) d_{ijk} B_j A_k |E_o|^2 B_i \quad (3-5-6)$$

where d_{eff} becomes:

$$d_{eff} = (2 - \delta_{jk}) d_{ijk} B_j A_k B_i \quad (3-5-7)$$

We are going to set up our experiment with type I interaction using BBO. I will calculate d_{eff} for all possible interactions. Then I will narrow it down to our special case of interaction. Recalling the electric susceptibility of BBO Eq. (2-3-14), we can find d_{eff} for any possible nonvanishing d_{ijk} . For calculating the total d_{eff} , we simply, add them together. Recall equation (3-3-21→23). Possible polarizations in three principal dimensions x, y, z for BBO crystal, considering $E_z = 0$ and type I phase matching, are

$$E_z = 0$$

$$P_x = 2d_{16}(E_x E_y), \quad (3-5-8)$$

$$P_y = d_{21}(E_x E_x) + d_{22}(E_y E_y), \quad (3-5-9)$$

$$P_z = d_{31}(E_x E_x) + d_{32}(E_y E_y), \quad (3-5-10)$$

We start with (3-5-8). It contains d_{16} (in the d_{in} tensor configuration) which means

$i = 1, n = 6$ or $i = 1, j = 1, k = 2$. Therefore, (2-5-5) for x direction becomes:

$$\begin{aligned} d_{effx}(BBO) &= (2 - \delta_{jk})d_{ijk}B_j A_k B_i = (2 - \delta_{12})d_{112}A_1 A_1 B_2 \\ &= 2d_{16}(\sin \phi)(-\cos \phi)(-\cos \phi \cos \theta_m) \\ &= 2d_{16} \cos^2 \phi \sin \phi \cos \theta_m \end{aligned} \quad (3-5-11)$$

For calculating d_{eff} in the y direction from (3-5-9),we write

$$\begin{aligned} d_{effy}(BBO) &= (2 - \delta_{jk})d_{ijk}B_j A_k B_i \\ &= (2 - \delta_{11})d_{211}A_1 A_1 B_2 + (2 - \delta_{22})d_{222}A_2 A_2 B_2 \\ &= d_{21} \sin \phi \sin \phi (-\sin \phi \cos \theta_m) + d_{22}(-\cos \phi)(-\cos \phi)(-\sin \phi \cos \theta_m) \\ &= -d_{21} \sin^3 \phi \cos \theta_m - d_{22} \cos^2 \phi \sin \phi \cos \theta_m \end{aligned} \quad (3-5-12)$$

In the z direction from (3-5-10) we have

$$\begin{aligned} d_{effz}(BBO) &= (2 - \delta_{jk})d_{ijk}B_j A_k B_i \\ &= (2 - \delta_{11})d_{311}A_1 A_1 B_3 + (2 - \delta_{22})d_{322}A_2 A_2 B_3 \\ &= d_{31} \sin \phi \sin \phi \sin \theta_m + d_{32}(-\cos \phi)(-\cos \phi) \sin \theta_m \\ &= d_{31} \sin^2 \phi \sin \theta_m + d_{32} \cos^2 \phi \sin \theta_m. \end{aligned} \quad (3-5-13)$$

The total d_{eff} would be:

$$\begin{aligned}
 d_{eff} &= d_{effx} + d_{effy} + d_{effz} \\
 &= (2d_{16} \cos^2 \phi \sin \phi \cos \theta_m - d_{21} \sin^3 \phi \cos \theta_m - d_{22} \cos^2 \phi \sin \phi \cos \theta_m + \\
 &\quad + d_{31} \sin^2 \phi \sin \theta_m + d_{32} \cos^2 \phi \sin \theta_m) \quad (3-5-14)
 \end{aligned}$$

Recalling the equation (1-3-17) for BBO symmetry

$$d_{16} = -d_{22} \quad , \quad d_{21} = -d_{22} \quad , \quad d_{31} = d_{32} \quad , \quad (3-5-15)$$

and replacing d_{16} with $-d_{22}$ and d_{21} with $-d_{22}$ in the Eq. (3-5-14), we have

$$\begin{aligned}
 d_{eff} &= (-2d_{22} \cos^2 \phi \sin \phi \cos \theta_m + d_{22} \sin^3 \phi \cos \theta_m - d_{22} \cos^2 \phi \sin \phi \cos \theta_m + \\
 &\quad + d_{31} \sin^2 \phi \sin \theta_m + d_{31} \cos^2 \phi \sin \theta_m) \quad (3-5-16)
 \end{aligned}$$

By using the relations

$$\sin^2 \phi + \cos^2 \phi = 1$$

$$\sin 3\phi = 3 \sin \phi - 4 \sin^3 \phi \quad ,$$

Eq. (3-5-16) becomes [13]:

$$d_{eff} = d_{31} \sin \theta_m - d_{22} \cos \theta_m \sin 3\phi \quad (3-5-17)$$

This is a general relation of the effective nonlinear coefficient using BBO crystal in type I phase matching. d_{31} and d_{22} have values of [13]

$$d_{31} = -0.16 \times 10^{-12} \text{ m/V} \quad \text{and} \quad d_{22} = 2.3 \times 10^{-12} \text{ m/V}. \quad (3-5-18)$$

Thus, for our experiment (SHG of 486 nm light at 243 nm UV beam) we calculate θ_m

(3-4-9)

$$\theta_m = 54.667^\circ \quad (3-5-19)$$

Because we have the option of cutting the BBO crystal to maximize d_{eff} , we cut it at $\phi = 90^\circ$. This way $\sin 3\phi$ gains its highest possible value. Finally we are able to calculate d_{eff} using (2-5-17) for our experiment:

$$\theta_m = 54.667^\circ; \quad \phi = 90^\circ.$$

$$\sin \theta_m = 0.8158 \quad \cos \theta_m = 0.5783 \quad \sin 3\phi = 1$$

$$d_{eff} = d_{31} \sin \theta_m - d_{22} \cos \theta_m \sin 3\phi = 1.40285 \times 10^{-12} \frac{m}{V} \quad (3-5-20)$$

Table III. lists d_{eff} .values for different wavelength using a BBO crystal in the type I interaction.

TABLE III. Calculated d_{eff} for the type I interaction using BBO.

$\lambda_\omega \Rightarrow \lambda_{2\omega}$	θ_m (Theoretical)	$d_{eff} (\times 10^{-12} \frac{m}{V})$
410nm \Rightarrow 205nm	85.535°	0.330
486nm \Rightarrow 243nm	54.667°	1.348
488nm \Rightarrow 244nm	54.288°	1.344
532nm \Rightarrow 266nm	47.529°	1.372
710nm \Rightarrow 355nm	32.913°	1.121
1064nm \Rightarrow 532nm	22.880°	0.633

The Walkoff Phenomenon

Up to now, we have been considering that propagation directions for the fundamental and the second harmonic waves are the same. This is true for both isotropic and anisotropic crystals. As we can see in Fig. 10. for a uniaxial crystal wave vectors for the fundamental and the second harmonic waves coincide.

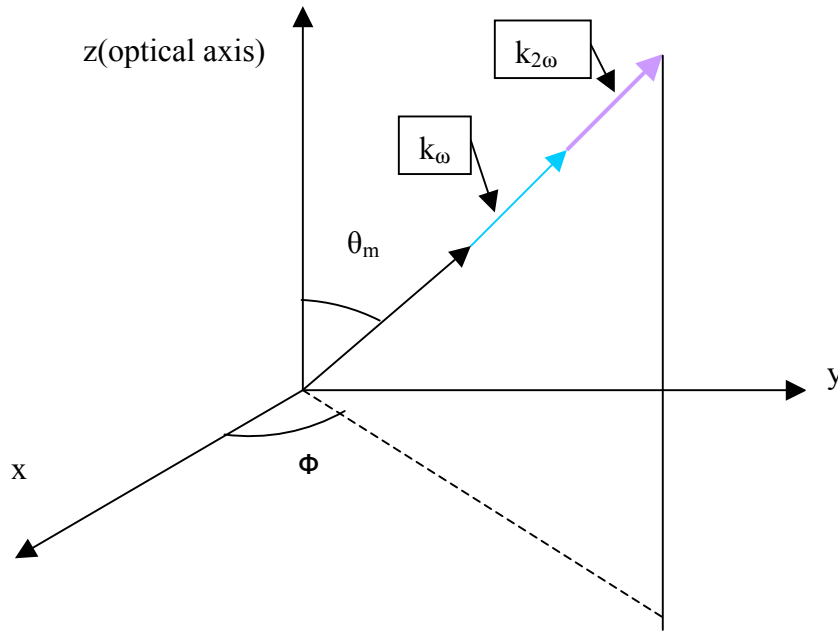


FIG. 10. k_ω (the blue vector refers to the fundamental blue laser light at 486 nm), $k_{2\omega}$ (the violet vector refers to the UV second harmonic laser at 243 nm).

Although vectors k_ω and $k_{2\omega}$ define the plane of constant phase for any laser beam in the crystal, directions of energy flow for the fundamental and the second harmonic are not the same in crystals like BBO. This comes from the fact that in anisotropic materials like BBO, the ordinary wave propagation k_ω is normal to the plane of $E_\omega \times H_\omega$ and $S_\omega = E_\omega \times B_\omega$, but for the extraordinary wave $k_{2\omega}$ is normal to

$E_{2\omega} \times H_{2\omega}$, but not normal to $S_{2\omega} = E_{2\omega} \times H_{2\omega}$. The segregation of the two flows of energy for the fundamental and the second harmonic beams is called walkoff or double refraction and the angle between these two vectors is called the walkoff angle ρ . This phenomenon can be seen in the Fig. 11.

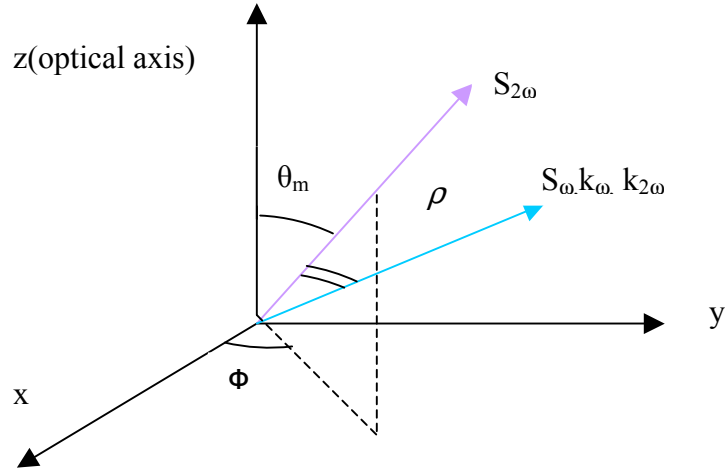


FIG. 11. The walk off angle between an ordinary an extraordinary wave in a negative uniaxial crystal.

To explain the cause of the double refraction or walkoff, we start with Maxwell's wave equation [11]:

$$\nabla \times (\nabla \times E) + \epsilon_0 \mu_0 \frac{\partial^2 E}{\partial t^2} + \mu_0 \frac{\partial P}{\partial t^2} + \mu_0 \frac{\partial J}{\partial t} = 0. \quad (3-6-1)$$

For a plane wave ($E \propto e^{i(k \cdot r - \omega t)}$), knowing $P = \epsilon_0 \chi E$ and that there is no current in the crystal ($J = 0$), (3-6-1) becomes:

$$\nabla \times (\nabla \times E) + \epsilon_0 \mu_0 \frac{\partial^2 E}{\partial t^2} + \mu_0 \epsilon_0 \chi \frac{\partial^2 E}{\partial t^2} = 0 \quad (3-6-2)$$

or

$$k \times (k \times E) + \epsilon_0 \mu_0 \omega^2 E + \mu_0 \epsilon_0 \chi \omega^2 \frac{\partial^2 E}{\partial t^2} = 0. \quad (3-6-3)$$

For an ordinary wave or on the principal axes χ is has a diagonal form of

$$\chi = \begin{pmatrix} \chi_{11} & 0 & 0 \\ 0 & \chi_{22} & 0 \\ 0 & 0 & \chi_{33} \end{pmatrix} \quad (3-6-4)$$

For an ordinary wave equation (3-6-3) the wave vector and energy flow $E \times H$ coincide. But for an extraordinary wave χ has the form of:

$$\chi = \begin{pmatrix} \chi_{11} & \chi_{12} & \chi_{13} \\ \chi_{21} & \chi_{22} & \chi_{23} \\ \chi_{31} & \chi_{32} & \chi_{33} \end{pmatrix} \quad (3-6-5)$$

Therefore, by plugging (3-6-5) into (3-6-3) we realize that $k \times (k \times E)$ has a component Along the E vector. This means that E is not perpendicular to k .

Considering the birefringence property of uniaxial anisotropic crystals, for an ordinary wave or in our experiment the fundamental 486 nm beam, the normal vector to the tangent is in the same direction of the wave vector. But for an extraordinary (second harmonic 243nm) the normal to the tangent is not in the same direction as the wave vector [13]. The walkoff angle for isotropic, positive and negative anisotropic crystals can be observed in Fig 12. By looking at Fig. 12 we can draw a relation for the walk off angle [13].

$$\rho(\theta_m) = \pm \arctan\left[\left(\frac{n_o}{n_e}\right)^2 \tan(\theta_m)\right] \mp \theta_m \quad (3-6-6)$$

where the upper sign is for negative crystals and the lower one is for positive crystals.

Now we can calculate walkoff angle for our case. Since the second harmonic wave is an extraordinary wave we need to have phase matching angle θ_m and indices of refraction

n_o, n_e at 243 nm wavelength.

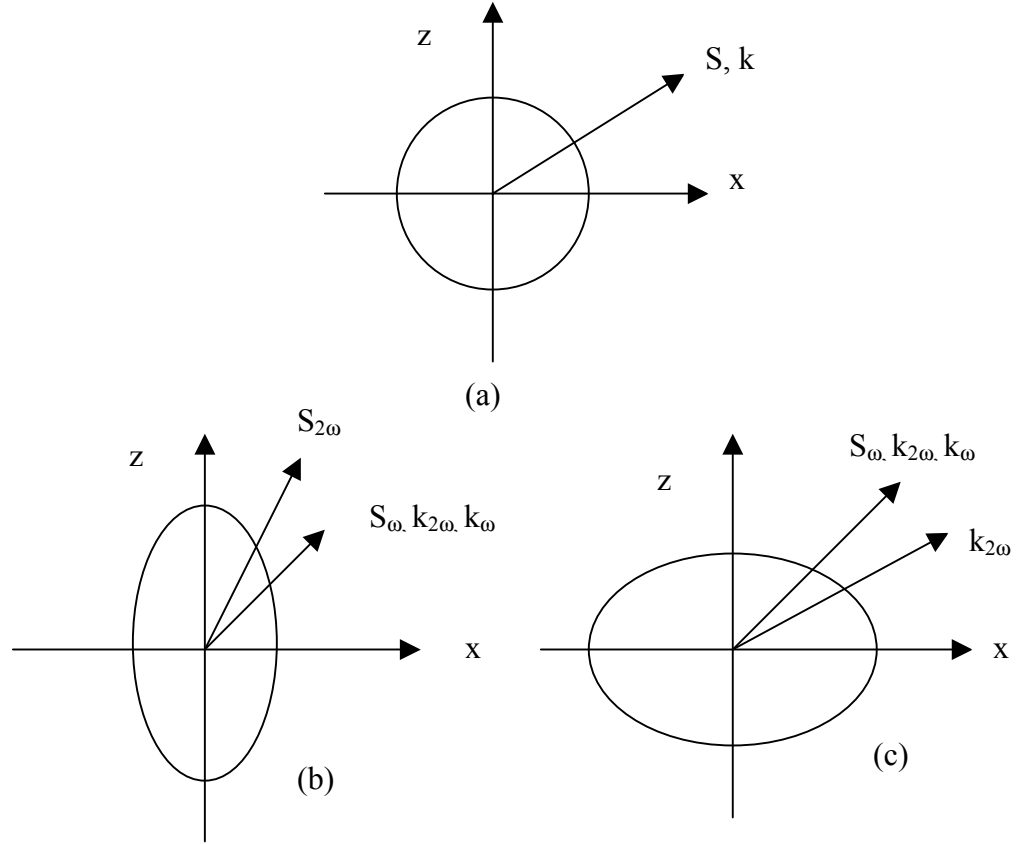


FIG. 12. (a) The ordinary wave vector in an isotropic materials, (b) the ordinary and extraordinary propagations in negative anisotropic crystals, (c) positive anisotropic crystals

Recalling Table 1. we had

$$\theta_m = 54.667^\circ \quad n_{o(243nm)} = 1.7851 \quad n_{e(243nm)} = 1.6332 .$$

Because BBO is a negative crystal, we have:

$$\begin{aligned} \rho(\theta_m) &= \arctan\left[\left(\frac{n_o}{n_e}\right)^2 \tan(\theta_m)\right] - \theta_m = \arctan\left[\left(\frac{1.7851}{1.6332}\right)^2 \tan(54.667^\circ)\right] - 54.667^\circ \\ &= 4.649^\circ \end{aligned} \quad (3-6-7)$$

This is the walkoff angle for an $(o + o \rightarrow e)$ interaction resulting from SHG of UV 243nm light from 486 nm blue light using BBO at room temperature operating.

From Eq. (3-6-6) we can conclude that if the phase matching θ_m has the value of 0° or 90° , the walkoff angle becomes zero. This comes from the fact that on the principal axes x, y, z waves are all ordinary. The phase matching with nonzero walkoff is called critical phase matching (CPM). Whereas, the phase matching with $\rho = 0$ is called noncritical phase matching (NCPM). Walkoff is a source of loss in the process of SHG. Since the double refraction or walkoff makes the beam elliptical., focusing of the beam becomes difficult. Therefore, noncritical phase matching has a lot more efficiency than critical phase matching. Because the walkoff segregates the fundamental and the second harmonic beams, a longer crystal experiences more elliptical divergence than a shorter crystal. The distance between the ordinary and the second harmonic energy flows caused by walkoff divergence can be calculated from

$$\delta = L \tan(\rho) \quad (3-6-8)$$

In our case, δ is calculated at

$$\begin{aligned} \delta &= (0.01) \tan(4.649^\circ) = 0.00081332 \text{ m} \\ &= 0.813 \text{ mm} \end{aligned}$$

Thus, the longer the length of crystal L , the wider the divergence distance δ . As can be seen in Fig. 13, the second harmonic becomes parallel to the fundamental after leaving the nonlinear medium. Calculated walkoff angles for type I phase matching at different frequencies of light using a 10 mm BBO crystal are listed in Table IV.

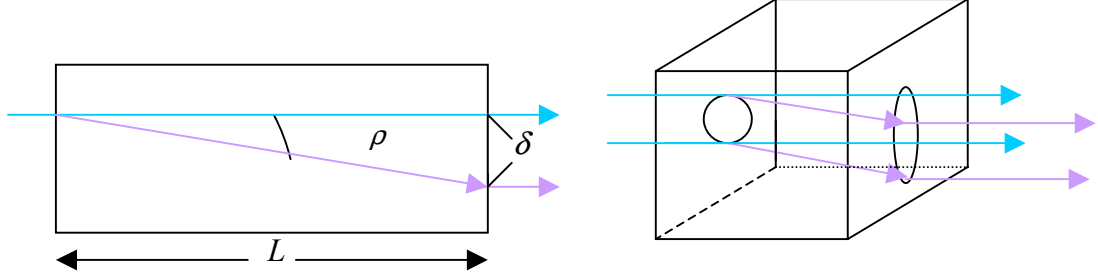


FIG. 13. The walkoff divergence between ordinary and extraordinary waves and shaping elliptical beams.

TABLE IV. Calculated walkoff angles for SHG of different frequencies using a 10 mm BBO crystal.

$\lambda_{\omega} \Rightarrow \lambda_{2\omega}$	θ_m (Theoretical)	ρ (walk off angle)
410nm \Rightarrow 205nm	85.535°	0.820°
486nm \Rightarrow 243nm	54.667°	4.649°
488nm \Rightarrow 244nm	54.288°	4.665°
532nm \Rightarrow 266nm	47.529°	4.796°
710nm \Rightarrow 355nm	32.913°	4.197°
1064nm \Rightarrow 532nm	22.880°	3.192°

The Single Pass Conversion Efficiency

The single pass conversion efficiency is a factor that enables us to predict the magnitude of the second harmonic power ($P_{2\omega}$) generated with respect to the fundamental beam power (P_{ω}) value passing through the nonlinear crystal only once.

The power conversion is not linear and has the form of:

$$P_{2\omega} \propto P_{\omega}^2 \quad (3-7-1)$$

We relate these two powers with a factor called the single pass conversion efficiency η , where

$$P_{2\omega} = \eta P_{\omega}^2. \quad (3-7-2)$$

To maximize η we have to have an efficient focusing of the laser beam into the crystal. A circular beam has a higher η . First, I consider the beam as a perfect circular beam. Then, I will include effects of elliptical shaping caused by the walkoff phenomenon. To achieve a desirable power output of UV laser at 243 nm for this experiment, one can focus a fundamental beam at 486 nm that should be optimized as a Gaussian beam or beam with TEM_{00} mode. The parameters concerning the focusing are beam waist or electric field radius W_o at $z = 0$, Rayleigh range z_R , length of crystal L , and confocal parameter b . The beam radius $W(z)$ and wavefront curvature $R(z)$ can be written as [9]:

$$W^2(z) = W_o^2 \left[1 + \left(\frac{z}{z_R} \right)^2 \right], \quad (3-7-3)$$

$$R(z) = z \left[1 + \left(\frac{z_R}{z} \right)^2 \right], \quad (3-7-4)$$

$$b = 2z_R = W_o^2 k_\omega, \quad (3-7-5)$$

where k_ω is the wave vector of the fundamental beam at 486nm for our experiment.

Gaussian focusing can be illustrated in the figure below.

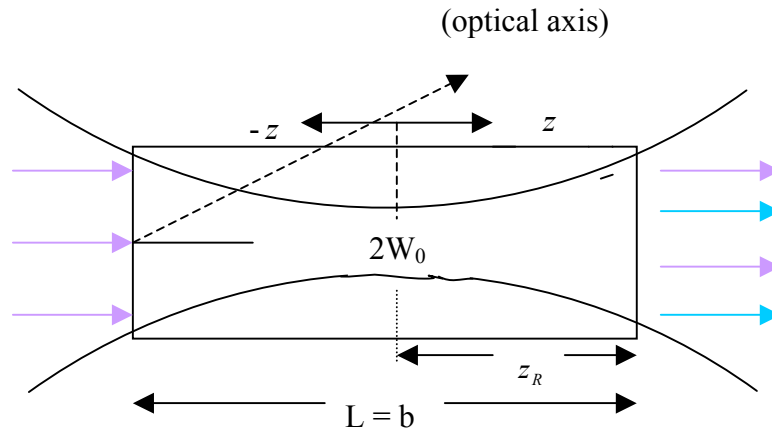


FIG. 14. A Gaussian beam focused in a crystal.

To optimize focusing the length of crystal L must be equal to the confocal parameter b .

The reason lies in the fact that for distances longer than z_R diffraction becomes considerably high. Therefore, to achieve maximum focusing, choosing z_R as $L = 2z_R$ is critical. In practice, the beam waist W_o can be adjusted by focusing lenses optimized into any length of crystal. For $z \ll z_R$, a Gaussian beam's electric field obeys [9]

$$E_{xy}(x, y) = E_0 e^{-\left(\frac{r^2}{W_o^2}\right)}, \quad (3-7-6)$$

where r is equal to $\sqrt{x^2 + y^2}$. We assume that z is the optical axis. Therefore, $E_z = 0$.

Following the discussion by R. L. Byer, et al [9] and G. D. Boyd, et. al. [15], the power of a beam with electric field like (3-7-4) can be written as

$$P = \frac{nc\mathcal{E}_0}{2} \int |E(x, y)|^2 dx dy. \quad (3-7-7)$$

By substituting the electric field from (3-7-6) into (3-7-7) we have:

$$\begin{aligned} P &= \frac{nc\mathcal{E}_0}{2} \int \left| E_0 e^{\left(-\frac{r^2}{W_0^2}\right)} \right|^2 dx dy \\ &= \frac{nc\mathcal{E}_0}{2} \int_0^\infty \int_0^{2\pi} \left| E_0 e^{\left(-\frac{r^2}{W_0^2}\right)} \right|^2 d\phi dr \\ &= \frac{nc\mathcal{E}_0}{2} |E_0|^2 \left(\frac{\pi W_0^2}{2} \right) \end{aligned} \quad (3-7-8)$$

The beam power above implies that the peak of laser intensity can be written as

$$I_0 = \frac{nc\mathcal{E}_0}{2} |E_0|^2. \quad (3-7-9)$$

The effective area of the Gaussian beam is

$$\sigma = \left(\frac{\pi W_0^2}{2} \right). \quad (3-7-10)$$

The second harmonic electric field $E_{2\omega}(x, y)$ made by the fundamental beam field

$E_\omega(x, y)$ can be expressed as [9]:

$$E_{2\omega}(x, y, L) = iK \int_0^L E_\omega^2(x, y) dz \quad (3-7-11)$$

where $K = \frac{\omega d_{eff}}{nc}$.

Recalling the nonlinear coefficient d_{eff} that was maximized by Eq. (3-5-17), the option of cutting the BBO crystal at $\phi = 90^\circ$ optimizes the efficiency. This means that the phase matching and the walkoff happen in the zy plane. A modified wave vector in the principal coordinate system is shown (for our application using a BBO crystal) in Fig. 15.

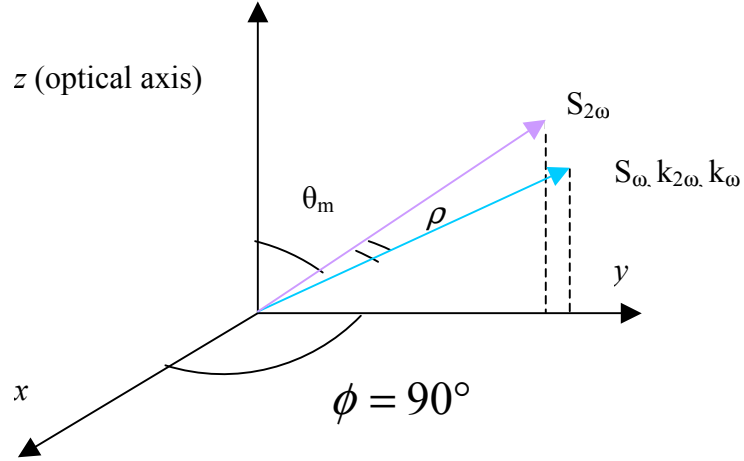


FIG. 15. The phase matching condition on the zy plane($\phi = 0$).

By translating the coordinates to

$$x = x',$$

$$\text{and} \quad y = y' + \rho(L - z') \quad (3-7-12)$$

$E_{2\omega}$ (3-7-11) becomes:

$$E_{2\omega}(x, y, L) = iK \int_0^L E_{\omega}^2(x, y - \rho(L - z')) dz \quad (3-7-13)$$

Writing E_{ω} (3-7-6) in two dimensions gives

$$E_{\omega} = E_{0\omega} e^{\left(-\frac{(x'+y')^2}{w_{\omega}^2}\right)}, \quad (3-7-14)$$

where W_ω is the beam waist for the fundamental wave. By this definition, (3-7-13) becomes:

$$E_{2\omega}(x, y, L) = \left(-\frac{2x}{W_\omega^2} \right) iKE_{0\omega}^2 \int_0^L e^{\left(-\frac{2}{W_\omega} [y - \rho(L-z')] \right)} dz' \quad (3-7-15)$$

By normalizing coordinates again using [16]

$$\begin{aligned} u &= \sqrt{2} \frac{y - \rho L}{W_\omega}, \\ \tau &= \sqrt{2} \frac{\rho z'}{W_\omega}, \\ t &= \sqrt{2} \frac{\rho L}{W_\omega}, \end{aligned} \quad (3-7-16)$$

and defining the function $F(u, t)$ as

$$F(u, t) = \frac{1}{t} \int_0^t e^{-(u+\tau)^2} d\tau, \quad (3-7-17)$$

Eq. (3-7-13) becomes:

$$E_{2\omega}(x, y, L) = ikKLE_{0\omega} \left(e^{-\frac{2x^2}{W_\omega^2}} \right) F(u, t). \quad (3-7-18)$$

$F(u, t)$ contains effects caused by walkoff. For example, if $\rho = 0$ in the critical phase matching regime (3-7-18) becomes:

$$\begin{aligned} F(u, t, \rho = 0) &= e^{-\left(\frac{2y^2}{W_\omega^2} \right)} \\ E_{2\omega}(x, y, L) &= iKLE_{0\omega} \left(e^{-\frac{2(x+y)^2}{W_\omega^2}} \right) \end{aligned} \quad (3-7-19)$$

Defining an aperture length parameter L_a can make the walkoff effect more understandable:

$$L_a = \frac{\sqrt{\pi} W_\omega}{\rho} \quad (3-7-20)$$

where L_a is the walkoff limit interaction length [15]. With this definition t becomes:

$$t = \sqrt{2\pi} \frac{L}{L_a} \quad (3-7-21)$$

Using (3-7-7), for calculating the total power of the second harmonic generated beam, we have:

$$P_{2\omega} = \frac{n c \epsilon_0}{2} \int_{-\infty-\infty}^{+\infty+\infty} |E_{2\omega}(x, y, L)|^2 dx dy \quad (3-7-22)$$

By substituting $E_{2\omega}$ from (3-7-18) into (3-7-22) and assuming

$$\int_0^\infty e^{-(ax)^2} = \frac{\sqrt{\pi}}{2a},$$

we can show:

$$P_{2\omega} = \frac{nc\epsilon_0}{2} K^2 E_\omega^4 \frac{\sqrt{\pi} W_\omega}{2} L^2 \int_{-\infty}^{+\infty} F^2(u, t) dy \quad (3-7-23)$$

If $K = \frac{\omega d_{eff}}{nc}$, (3-7-23) can be written as:

$$P_{2\omega} = \frac{nc\epsilon_0}{2} \left(\frac{\omega d_{eff}}{nc} \right)^2 E_\omega^4 \frac{\sqrt{\pi} W_\omega}{2} L^2 \int_{-\infty}^{+\infty} F^2(u, t) dy \quad (3-7-24)$$

From (3-7-8) P_ω is:

$$P_{\omega} = \frac{nc\epsilon_0}{2} |E_{\omega}|^2 \left(\frac{\pi W_{\omega}^2}{2} \right) \quad (3-7-25)$$

Eq. (3-7-24) has been modified by [15], [9] to:

$$\frac{P_{2\omega}}{P_{\omega}^2} = \left(\frac{2\omega^2 d_{eff}^2 k_{\omega} L}{\pi \epsilon_0 n_{0\omega}^2 n_{e2\omega} c^3} \right) h(B, \xi) \quad (3-7-26)$$

where ξ is the focusing parameter:

$$\xi = \frac{L}{b} \quad (3-7-27)$$

and B is the walk off parameter:

$$B = \frac{1}{2} \rho \sqrt{k_{\omega} L} \quad (2-7-28)$$

It has been proven that in the range of $10 < B < 20$, for a value of $\xi = 1.39$ the factor $h(B, \xi)$ has its maximum value possible [5]. The factor $h(B, \xi)$ is the Kleinman focusing parameter which determines the losses through walkoff. Using the Mathematica software, we have plotted h as a function of B in the figure below:

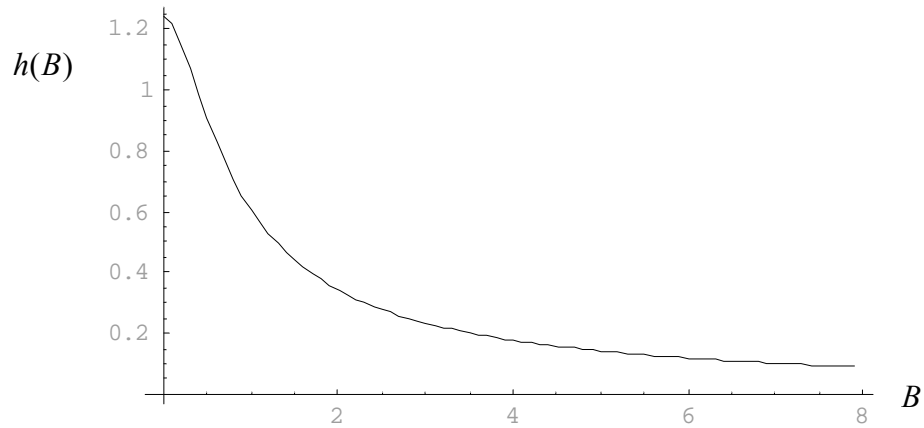


FIG. 16. The $h(B)$ factor as a function of B , for $B < 8$.

A lower value of $h(B, \xi)$ gives a higher loss by walkoff and vice versa. $h(B, \xi)$ as a function of B for $B < 50$ has been fitted to the relation below [17]:

$$h(B) \cong \frac{B + 0.568}{1.421B^2 + 0.791B + 0.537} \quad (-7-29)$$

For a zero walkoff in the critical phase matching regime $\rho=0$, $B=0$, $h(B=0)$ has a maximum of [15]:

$$h_{\max}(B=0)=1.068.$$

The $h(B, \xi)$ factor decreases rapidly with increasing B or walkoff parameter.

For our experiment, B can be calculated at

$$B = \frac{1}{2} \rho \sqrt{k_{\omega} L} = 18.9084 \quad (3-7-30)$$

The corresponding $h(B, \xi)$ factor to $B = 18.9084$, using Eq. (3-7-29), is

$$h(B = 18.9084, \xi = 1.39) \cong \frac{B + 0.568}{1.421B^2 + 0.791B + 0.537} = 0.0372014. \quad (3-7-31)$$

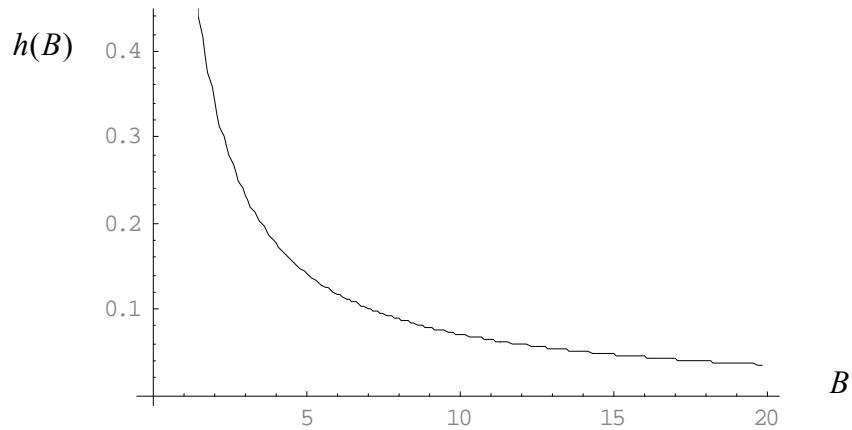


FIG. 17. The $h(B)$ factor as a function of B , for $B < 20$.

Finally, the single pass conversion efficiency η using (3-7-26) can be written as

$$\eta = \frac{P_{2\omega}}{P_{\omega}^2} = \left(\frac{2\omega^2 d_{eff}^2 k_{\omega} L}{\pi \epsilon_0 n_{0\omega}^2 n_{e2\omega} c^3} \right) h(B, \xi) \quad (3-7-32)$$

The single pass conversion efficiency for frequency doubling of 486 nm light for type I phase matching using a 10 mm long BBO crystal at room temperature is calculated to be

$$\eta = \frac{P_{2\omega}}{P_{\omega}^2} = \left(\frac{2\omega^2 d_{eff}^2 k_{\omega} L}{\pi \epsilon_0 n_{0\omega}^2 n_{e2\omega} c^3} \right) h(B, \xi) = 0.000134464 \frac{1}{W}. \quad (3-7-33)$$

Now we are able to calculate second harmonic power $P_{2\omega}$ at 243 nm UV laser for any given power of the fundamental laser beam P_{ω} at 486 nm. If the fundamental laser beam can provide $P_{\omega} = 50 \text{ mW}$, the corresponding $P_{2\omega}$ would be

$$\begin{aligned} P_{2\omega}(\lambda_{\omega} = 243 \text{ nm}) &= \eta P_{\omega}^2(\lambda_{2\omega} = 486 \text{ nm}) = (0.000134464)(0.05)^2 \\ &= 0.00000033616 \text{ W} \\ &= 0.33 \text{ } \mu\text{W} \end{aligned} \quad (3-7-34)$$

The laser power at 243 nm resulting from a single pass operation is extremely low. As can be seen in Table V., the single conversion efficiency η of the BBO crystal is not high due to the small value of the nonlinear coefficient d_{eff} . To compensate this energy loss through the second harmonic process, the use of a buildup cavity is an option.

In the next chapter, we will place the crystal in a standing build up cavity to amplify the output power for the second harmonic light at 243 nm.

TABLE V. Calculated θ_m , d_{eff} , ρ , B , $h(B)$ and η for SHG of different frequencies using a 10 mm BBO crystal in the room temperature operation.

$\lambda_\omega \Rightarrow \lambda_{2\omega}$	θ_m	$d_{eff} (\frac{pm}{V})$	ρ	B	$h(B)$	$\eta (\times 10^{-4} \frac{1}{W})$
410 nm \Rightarrow 205 nm	85.535°	0.330	0.820°	3.643	0.189	0.623
486 nm \Rightarrow 243 nm	54.667°	1.414	4.649°	18.931	0.037	1.348
488 nm \Rightarrow 244 nm	54.288°	1.402	4.665°	18.908	0.037	1.344
532 nm \Rightarrow 266 nm	47.529°	1.606	4.796°	18.615	0.037	1.372
710 nm \Rightarrow 355 nm	32.913°	1.933	4.197°	14.059	0.049	1.121
1064 nm \Rightarrow 532 nm	22.880°	2.080	3.192°	8.711	0.080	0.633

CHAPTER 4

BUILDUP CAVITIES

Configurations of Buildup Cavities Using Mirrors

In the last chapter, we calculated the single pass conversion efficiency of SHG of 486 nm light to produce a UV laser light at 243 nm . But the final output power of UV light was very low. A buildup cavity can amplify this power. For our spectroscopy purpose, we need at least 2 mW power at 243 nm . If the BBO crystal is placed between two highly reflective mirrors, the fundamental light can bounce back and forth and start building up the power of light.

There are two common buildup cavity configurations that have been used successfully for resonators and optical amplifiers using mirrors. They are called standing wave and ring cavities.

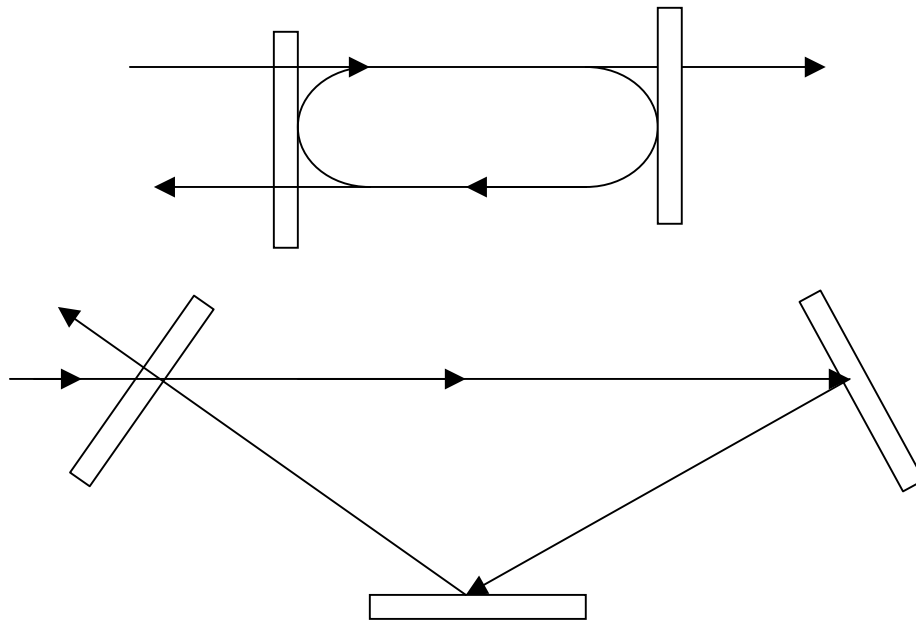


FIG. 18. (a) A typical standing cavity (b) A typical ring cavity

In a standing wave cavity power can get reflected from the input mirror back to the laser diode (LD). On the other hand, in a ring cavity the reflected beam and build up beam leave the cavity with different angles from incident beam and don't go back to the fundamental laser system. This makes a ring cavity more practical.. The standing cavity configuration is simpler to align than the ring cavity. For this reason, I would like to use a standing wave cavity. The feedback power to LD can be minimized using an optical isolator.

Standing Buildup Cavities

By placing the BBO crystal between two mirrors the fundamental beam can be amplified, which means the SHG beam will be improved. The job of frequency doubling and amplification can happen at same time.

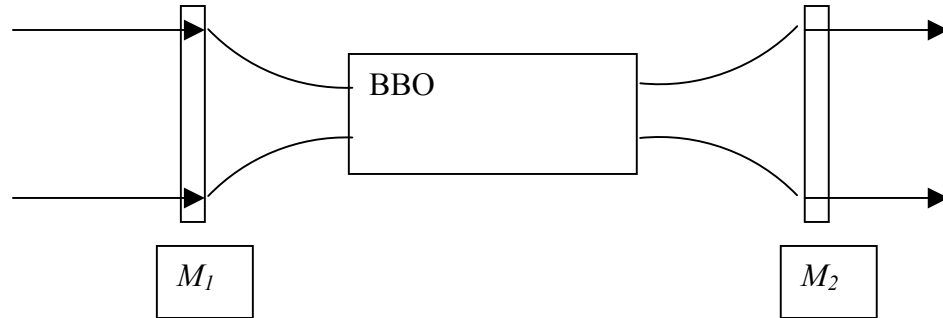


FIG. 19. A build up cavity with crystal placed inside for SHG and power amplification purpose.

The mirror M_1 has a reflectivity of R_1 and a transmission of T_1 such that

$$T_1 + R_1 = 1. \quad (4-2-1)$$

If the electric field for the fundamental wave is E_ω with power of P_ω , the circulating electric field inside the cavity is E_{cir} with power of P_{cir} and the second harmonic electric field is $E_{2\omega}$ with power of $P_{2\omega}$, we can write:

$$P_{2\omega} = \eta P_{cir}^2 \quad (4-2-2)$$

$$P_{2\omega} = \beta P_\omega \quad (4-2-3)$$

$$BU = \frac{P_{cir}}{P_\omega} \quad (4-2-4)$$

where BU is called build up factor and β is overall power efficiency. The BU factor for a buildup cavity can be defined as a function of transmission of the mirror 1 (T_1) and total loss L in the cavity [21]:

$$BU = \frac{T_1}{(1 - \sqrt{1 - L} \sqrt{1 - T_1})^2} \quad (4-2-5)$$

$$\text{with} \quad L = L_\omega + L_{2\omega} \quad (4-2-6)$$

where $L_\omega, L_{2\omega}$ are the fundamental and the second harmonic fractional round trip power losses. For $T_1 \ll 1$ and $L \ll 1$, (4-2-5) becomes:

$$BU = \frac{4T_1}{(T_1 + L)^2} \quad (4-2-7)$$

Eq. (4-2-5) can be rewritten as:

$$BU = \frac{T_1}{(1 - \sqrt{1 - L_\omega - L_{2\omega}} \sqrt{1 - T_1})^2} \quad (4-2-8)$$

From equations (4-2-2), (4-2-3) and (4-2-4) we can write:

$$P_{2\omega} = \eta(BUP_{\omega})^2, \quad (4-2-9)$$

and

$$\beta = \frac{T_1^2 \eta P_{\omega}}{[1 - \sqrt{1 - T_1} \sqrt{1 - L_{\omega} - L_{2\omega}}]}. \quad (4-2-10)$$

In the equation above $L_{2\omega}$ must be calculated. However, L_{ω} is the bulk loss for the fundamental wave and can be calculated using the absorption coefficient α_1 for 486 nm light in the BBO crystal. Since $P_{2\omega} = \eta P_{cir}^2$, $L_{2\omega}$ can be defined as

$$L_{2\omega} = \frac{P_{2\omega}}{P_{cir}}. \quad (4-2-11)$$

Assuming an absorption coefficient α for P_{cir} , P_{cir} is going to be the function of

$$P_{cir}(z) = P_{cir} e^{-\alpha z}. \quad (4-2-12)$$

As it can be assumed that $P \propto E^2$, Eq. (4-2-12) becomes:

$$E_{cir}^2(z) = E_{cir}^2 e^{-\alpha z}. \quad (4-2-13)$$

By differentiating (4-2-12) we write:

$$\frac{dP_{cir}(z)}{dz} = -\alpha P_{cir} e^{-\alpha z} \quad (3-2-14)$$

From conservation energy and power at any point in the crystal we have

$$P_{cir} + P_{2\omega} = \text{constant} \quad \text{or} \quad E_{cir}^2 + E_{2\omega}^2 = \text{constant}. \quad (4-2-15)$$

By differentiating both sides of the equation above we can write:

$$dE_{2\omega}(z) = \alpha E_{cir}^2(z) dz \quad (4-2-16)$$

$$dE_{cir}(z) = \alpha E_{cir}(z) E_{2\omega} dz \quad (4-2-17)$$

Using the Mathematica software, I have found two solutions for the coupled differential equations (4-2-16,17):

$$E_{2\omega}(z) = E_{cir} \tanh(\alpha z)$$

$$E_{cir}(z) = E_{cir} \sqrt{1 - \tanh^2(\alpha z)} \quad (4-2-18)$$

where the boundary conditions of $P_{cir} \alpha^2 L^2 = \eta P_{cir}^2$ and $BU = \frac{P_{cir}}{P_\omega}$ imply that

$$\alpha = \frac{\sqrt{\eta B U P_\omega}}{L} \quad (4-2-19)$$

where L is the length of crystal. Thus, $L_{2\omega}$ (4-2-11) for the total length of crystal $z = L$ becomes:

$$L_{2\omega} = \frac{P_{2\omega}}{P_{cir}} = \frac{E_{cir}^2 \tanh^2(\alpha z)}{E_{cir}^2} = \tanh^2 \sqrt{\eta B U P_\omega} \quad (4-2-20)$$

Now, we can rewrite (4-2-8) as

$$BU = \frac{T_1}{[1 - \sqrt{1 - L_\omega - \tanh^2(\sqrt{\eta B U P_\omega})} \sqrt{1 - T_1}]^2} \quad (4-2-21)$$

The overall conversion efficiency β (4-2-10) becomes:

$$\beta = \frac{T_1 \tanh^2 \sqrt{\eta B U P_\omega}}{[1 - \sqrt{1 - T_1} \sqrt{1 - L_\omega - \tanh^2 \sqrt{\eta B U P_\omega}}]^2} \quad (4-2-22)$$

Because P_ω , L_ω , and η are constant, we can optimize the η and β by using an appropriate input coupler mirror with optimized transmission coefficient T_1 . To do so, we have plotted the overall efficiency β as a function of T_1 for our application

($P_\omega = 0.05 \text{ W}$, $L_\omega = 0.01$ for BBO [13], $\eta = 0.0001344 \frac{1}{W}$, $L = 10 \text{ mm}$ BBO). We have found a maximum for β at $T_l = 0.011$.

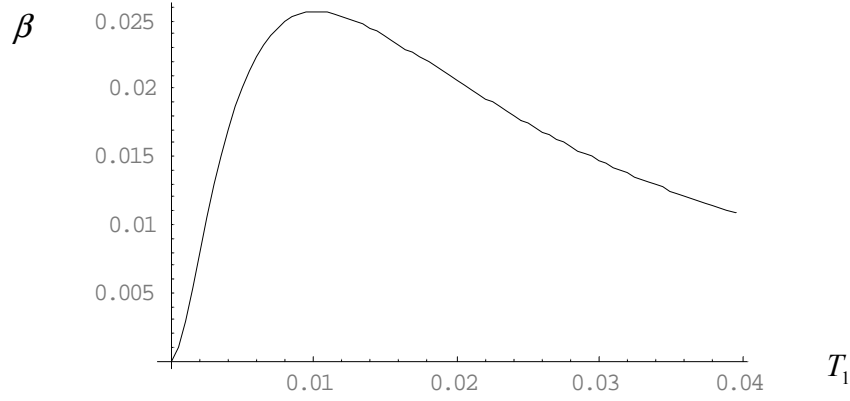


FIG. 20. Plotted β as a function of T_l (at $T_l=0.011$ there is a peak for β)

Therefore, to maximize the power of the second harmonic beam at 243 nm we need to use an input mirror with 1.1% transmission or 98.9% reflection for 486 nm light. With these parameters, finally, we can predict the value of output power of the second harmonic generation. The build up factor becomes:

$$BU = \frac{T_l}{[1 - \sqrt{1 - L_\omega - \tanh^2(\sqrt{\eta B U P_\omega})} \sqrt{1 - T_l}]^2} = 94.0314 \quad (4-2-23)$$

and overall conversion efficiency:

$$\beta = \frac{T_l \cdot \tanh^2 \sqrt{\eta B U P_\omega}}{[1 - \sqrt{1 - T_l} \sqrt{1 - L_\omega - \tanh^2 \sqrt{\eta B U P_\omega}}]^2} = 0.0593926 \quad (4-2-24)$$

Therefore we can calculate from (4-2-3):

$$\begin{aligned} P_{2\omega} &= \beta P_\omega = (0.0593926)(0.05) = 0.00296963 \text{ W} \\ &= 2.96963 \text{ mW} \end{aligned} \quad (4-2-25)$$

This is the amplified UV light power at 243 nm generated by SHG of a 486 nm laser beam using a 10 mm BBO crystal inside a standing wave buildup cavity.

To avoid reflection of light from the surfaces of the crystal, we can cut the crystal at the Brewster angle. The Brewster angle is the angle of which a light beam propagates across the boundary between two different media without being reflected. At the Brewster angle, the refracted ray and the reflected ray are normal to each other.

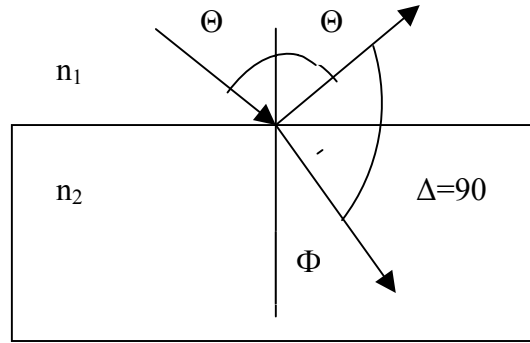


FIG. 21. The reflection and the refraction of a light beam at a boundary.

Writing Snell's law for a boundary such as shown in FIG. 21. we have

$$n_1 \sin \Theta = n_2 \sin \Phi . \quad (4-2-26)$$

Since

$$\Phi + \Delta + \Theta = 180^\circ \quad (4-2-27)$$

The Brewster condition requires:

$$\Delta = 90^\circ , \quad \Phi + \Theta = 90^\circ \quad (4-2-28)$$

For our application light propagates from the air ($n_1 = 1$) into the BBO crystal as an ordinary wave with $n_o(\lambda = 486 \text{ nm}) = 1.6796$ using a BBO crystal. Therefore, Snell's

law becomes:

$$\begin{aligned} n_{air} \sin \Theta_B &= n_{o486nm} \sin \Phi = n_{o486nm} \sin(90^\circ - \Theta_B) \\ &= n_{o486nm} \cos \Theta_B \quad (4-2-29) \end{aligned}$$

Therefore, the Brewster angle for BBO at 486 nm becomes:

$$\Theta_B = \tan^{-1}\left(\frac{n_{o486nm}}{n_{air}}\right) = \tan^{-1}\left(\frac{1.6796}{1}\right) = 59.231^\circ \quad (4-2-30)$$

Finally, the build up cavity with Brewster cut BBO has the configuration of:

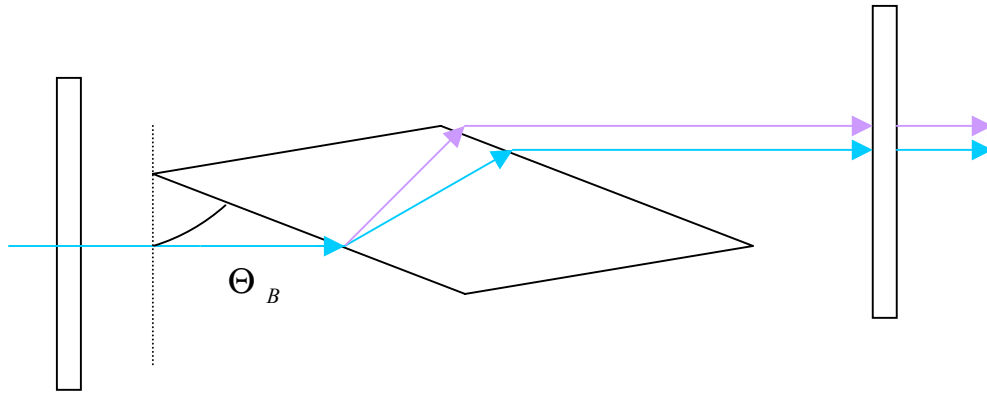


FIG. 22 The Brewster cut BBO in a standing buildup cavity for SHG purpose. The Blue lines show the fundamental beam or the blue laser at 486 nm. The Violet lines are propagation direction of second harmonic 243 nm UV laser.

With this configuration the theoretical values promise the overall conversion efficiency of

$$\beta = \frac{P_\omega}{P_{2\omega}} = \frac{0.00296963}{.05} = 0.059 = 5.9\% \quad (4-2-31)$$

for our application, which seems to meet the desired power conversion for our purpose.

REFERENCES

- [1] T. H. Maiman, *Nature* **187**, 493 (1960).
- [2] P. Franken, A. Hills, C. Peters, and G. Weinrich, *Phys. Rev. Lett.* **7**, 118 (1961).
- [3] T. Sasaki, Y. Mori, M. Yoshimura, Y. K. Yap, and T. Kamimura, *Mater. Sci. Eng.* **3**, 1 (2000).
- [4] M. S. Fee, A. P. Mills, S. Chu, E. D. Shaw, K. Danzman, R. J. Chichester and D. M. Zuckerman, *Phys. Rev. Lett.* **70**, 1397 (1992).
- [5] A. Steinbach, M. Rauner, F. C. Cruz, J. C. Brgquist, *Opt. Comm.* **123**, 207 (1996).
- [6] C. Zimmermann, V. Vuletic, A. Hemmerich and T. W. Hansch, *Phys. Rev. Lett.* **65**, 2318 (1995).
- [7] S. Sayama, M. Ohitsu, *Opt. Comm.* **145**, 95 (1998).
- [8] F. Zernike, and J. E. Midwinter, Applied Nonlinear Optics, (John Wiley & Sons, New York 1973), p 2.
- [9] P. G. Harper, and B. Wherrett, Nonlinear Optics, (Academic Press, New York 1977).
- [10] A. Yariv, and P. Yeh, Optical Waves in Crystals, (John Wiley & Sons, New York, 1984), p. 506.
- [11] G. Fowles, Introduction to Modern Optics, 2nd ed. (Holt, Rinehart and Winston, 1975), p. 170.
- [12] J. D. Jackson, Classical Electrodynamics, 3rd, (John Wiley & Sons, New York, 1999) p. 237.
- [13] V. Dmitriev, G. G. Gurzadyan, and D. N. Nikogosyan, Handbook of Nonlinear Optical Crystals, 3rd ed. (Springer, New York, 1999), p. 6.
- [14] D. Eimerl, L. Davis, S. Velsko, E. K. Graham, and A. Zalkin, *J. Appl. Phys.* **62**, 1968 (1987).
- [15] G. D. Boyd, and D. A. Klienman, *J. Appl. Phys.* **39**, 3597 (1968).

- [16] G. D. Boyd, A. Ashkin, J. M. Dziedzic, and D. A. Kleinman, Phys. Rev. **B7**, A1305 (1965).
- [17] J. Hald, Opt. Comm. **197**, 169 (2001).
- [18] S. Bourzeix, B. de Beauvoir, F. Nez, F. de Tomasi, L. Julien, and F. Biraben, Opt. Comm. **133**, 239 (1997).
- [19] X. Xinan, and Y. Shuzhong Chinese Phys. Lett. **13**, 175 (1986).
- [20] J. Y. Huang, J. Y. Zhang, Y. R. Shen, C. Chen, and B. Wu, Appl. Phys. Lett. **57**, 1961 (1990).
- [21] A. Siegman, Lasers, (University Science Books, California, 1986), p.431.